Molecular Evolution and Selection Patterns of Plant F-Box Proteins with C-Terminal Kelch Repeats[1][W][OA]

Nadine Schumann[2], Aura Navarro-Quezada[2], Kristian Ullrich, Carsten Kuhl, and Marcel Quint*

Independent Junior Research Group (N.S., K.U., M.Q.) and Department of Stress and Developmental Biology (A.N.-Q., C.K.), Leibniz Institute of Plant Biochemistry, 06120 Halle, Germany

The F-box protein superfamily represents one of the largest families in the plant kingdom. F-box proteins phylogenetically organize into numerous subfamilies characterized by their carboxyl (C)-terminal protein-protein interaction domain. Among the largest F-box protein subfamilies in plant genomes are those with C-terminal kelch repeats. In this study, we analyzed the phylogeny and evolution of F-box kelch proteins/genes (FBKs) in seven completely sequenced land plant genomes including a bryophyte, a lycophyte, monocots, and eudicots. While absent in prokaryotes, F-box kelch proteins are widespread in eukaryotes. Nonplant eukaryotes usually contain only a single *FBK* gene. In land plant genomes, however, *FBK*s expanded dramatically. *Arabidopsis thaliana*, for example, contains at least 103 F-box genes with well-conserved C-terminal kelch repeats. The construction of a phylogenetic tree based on the full-length amino acid sequences of the FBKs that we identified in the seven species enabled us to classify *FBK* genes into unstable/stable/superstable categories. In contrast to superstable genes, which are conserved across all seven species, kelch domains of unstable genes, which are defined as lineage specific, showed strong signatures of positive selection, indicating adaptational potential. We found evidence for conserved protein features such as binding affinities toward *A. thaliana* SKP1-like adaptor proteins and subcellular localization among closely related FBKs. Pseudogenization seems to occur only rarely, but differential transcriptional regulation of close relatives may result in subfunctionalization.

The process of protein degradation is an important posttranslational regulatory mechanism. It is integral to cellular homeostasis by removing nonfunctional and misfolded proteins and allows living organisms to adapt to changing environments by providing fast responses to intracellular signals. A major player in this process is the ubiquitin/26S proteasome system, which is responsible for selective degradation of many intracellular proteins (Stone and Callis, 2007; Vierstra, 2009). Proteins destined for degradation are modified by covalent attachment of multiple ubiquitin moieties. The polyubiquitinated substrates are recognized and degraded by the 26S proteasome, while the ubiquitin molecules are recycled. The ubiquitination process includes three steps. First, the ubiquitin is activated by a ubiquitin-activating enzyme (E1). Subsequently, the ubiquitin is transferred to the ubiquitin-conjugating enzyme (E2). Finally, the transfer of activated ubiquitin to the target protein is catalyzed by a ubiquitin ligase (E3; Stone and Callis, 2007). The selective components of this cascade are the E3 ubiquitin ligases. These structurally diverse enzymes occur as monomers or in multimeric complexes. The various E3 families are classified according to their mode of action and subunit composition (Mazzucotelli et al., 2006). The most prevalent E3 ubiquitin ligases in plants are the Skp1-Cullin-F-box (SCF) protein complexes. The SCF complex is formed by an S-phase kinase-associated protein 1 (SKP1), Cullin 1 (CUL1), RING-box 1 (RBX1), and an F-box protein. While CUL1 functions as a scaffold, SKP1 mediates the connection between CUL1 and the F-box subunit. RBX1 serves as a docking port for the ubiquitin-conjugating E2 enzyme. The F-box protein mediates the specificity of the SCF complex by selectively recruiting target proteins via a protein-protein interaction domain (Cardozo and Pagano, 2004). The *Arabidopsis thaliana* genome (The Arabidopsis Information Resource, TAIR9 version) contains a single *CUL1* gene (Risseeuw et al., 2003), 19 functional genes coding for *A. thaliana* SKP1-like proteins (ASKs; Takahashi et al., 2004), and approximately 700 F-box genes (Gagné et al., 2002). The huge amount of combinatorial possibilities is evident and seems to be dominated by the hundreds of F-box proteins within the plant genomes assessed so far. Whereas human, *Drosophila melanogaster*, and *Schizosaccharomyces pombe* genomes contain 68 (Jin et al., 2004), 33 (Ou et al., 2003), and 18 (Hermand, 2006) F-box genes, respectively, this number is much higher in plants. The only species for which numbers comparable to plants were reported seems to be *Caenorhabditis elegans*, with approxi-

[1] This study was supported by the Deutsche Forschungsgemeinschaft (grant no. SFB648 to M.Q.).

[2] These authors contributed equally to the article.

* Corresponding author; e-mail mquint@ipb-halle.de.

The author responsible for distribution of materials integral to the findings presented in this article in accordance with the policy described in the Instructions for Authors (www.plantphysiol.org) is: Marcel Quint (mquint@ipb-halle.de).

[W] The online version of this article contains Web-only data.

[OA] Open Access articles can be viewed online without a subscription.

www.plantphysiol.org/cgi/doi/10.1104/pp.110.166579

mately 520 F-box proteins (Thomas, 2006). To date, for *A. thaliana*, *Oryza sativa*, *Populus trichocarpa*, and *Vitis vinifera*, 692, 779, 337 (Xu et al., 2009), and 156 (Yang et al., 2008) F-box genes were identified, respectively. Even for the model plant *A. thaliana*, less than 5% of the F-box proteins have been functionally characterized, but F-box proteins with known functions suggest that they play prominent roles in multiple physiological processes in plants, such as responses to various hormones (Ruegger et al., 1998; Xu et al., 2002; Guo and Ecker, 2003; Dill et al., 2004; Binder et al., 2007), the circadian clock and photomorphogenesis (Han et al., 2004; Fukamatsu et al., 2005; Kim et al., 2007; Sawa et al., 2007), flower development (González-Carranza et al., 2007; Chae et al., 2008), senescence (Woo et al., 2001), and defense responses (Kim and Delaney, 2002).

F-box proteins share a well-conserved approximately 50-amino acid F-box motif at their N terminus (Kipreos and Pagano, 2000). Furthermore, most F-box proteins contain a C-terminal protein-protein interaction domain, such as leucine-rich repeats (LRRs), kelch repeats, or F-box associated domains (Gagné et al., 2002; Xu et al., 2009). Phylogenetically, F-box proteins cluster according to their protein-protein interaction domains (Gagné et al., 2002), which putatively mediate binding to the corresponding target. One of these subfamilies is constituted by the F-box kelch proteins (FBKs), which contain C-terminal kelch repeats in addition to the N-terminal F-box. In plants, the subfamily of FBKs includes members with one to five kelch repeats. Proteins containing kelch repeat domains in the absence of an F-box are widespread and have been described for *A. thaliana*, human, *D. melanogaster*, *C. elegans*, and *S. pombe* (Prag and Adams, 2003; Leung et al., 2004; Mora-García et al., 2004). Such proteins typically include five to seven kelch repeats, which may form β-propellers, as shown by the crystal structure of the human kelch protein KEAP1 (Li et al., 2004). Given their rare occurrence in nonplant organisms and the fact that only a single nonplant FBK has been functionally described so far (Sun et al., 2009), FBK proteins seem to be rather plant specific. The *A. thaliana* genome codes for approximately 100 *FBK*s, four of which have been functionally characterized. ATTENUATED FAR-RED RESPONSE (AFR) is a positive regulator of phytochrome A-mediated light signaling (Harmon and Kay, 2003). ZEITLUPE (ZTL), FLAVIN-BINDING KELCH-REPEAT F-BOX1 (FKF1), and LOV KELCH PROTEIN2 (LKP2), which contain N-terminal PAS/LOV domains in addition to the F-box motif, are involved in photomorphogenesis and regulation of the circadian clock (Sawa et al., 2007; Demarsy and Fankhauser, 2009; Kim et al., 2010).

Representing one of the biggest protein families in *A. thaliana*, the F-box protein superfamily has been studied on a phylogenetic and evolutionary scale (Gagné et al., 2002; Yang et al., 2008; Xu et al., 2009). However, the analysis of up to 700 genes/proteins can only provide a glimpse on the evolution, phylogenetics, and functional divergence of the various distinct subfamilies. Several of these subfamilies are by themselves larger than most other known gene families in plants. To get a better understanding of how single subfamilies evolved, we focused our attention on one of the biggest yet largely uncharacterized F-box subfamilies in *A. thaliana*, the FBKs. Due to nearly completely sequenced and annotated genomes, we were able to examine FBK families in the eudicots *A. thaliana*, *P. trichocarpa*, and *V. vinifera*, the monocots *O. sativa* and *Sorghum bicolor*, the lycophyte *Selaginella moellendorffii*, and the bryophyte *Physcomitrella patens*. In this study, we first de novo identified FBKs by a combined approach using BLASTP and hidden Markov model (HMM)-based searches in the respective genomes. We then constructed phylogenetic trees and calculated K_a/K_s values to explore the evolutionary and selective forces acting on *FBK*s in plants. Lastly, expression patterns of *FBK* genes, subcellular localization, and ASK-binding patterns of selected FBK proteins in *A. thaliana* were investigated to assess potential functional conservation/diversification of closely related FBKs in land plants. Besides the evolutionary insights gained by this study, these data also provide a scaffold for future functional analysis of this large family of F-box proteins.

RESULTS

*FBK*s Expanded in Land Plant Genomes

To identify FBKs, we performed a BLASTP search against the annotated genomes of *A. thaliana* (*At*), *P. trichocarpa* (*Pt*), and *O. sativa* (*Os*) using species-specific consensus sequences derived from the full-length protein sequences of previously published FBKs (Gagné et al., 2002; Jain et al., 2007; Xu et al., 2009). Furthermore, we used an HMM-based search to identify additional FBKs in the aforementioned species as well as in the genomes of *V. vinifera* (*Vv*), *S. bicolor* (*Sb*), *S. moellendorffii* (*Sm*), and *P. patens* (*Pp*). In the eudicots *At*, *Vv*, and *Pt*, we identified 103, 36, and 68 FBKs, respectively. Thirty-nine and 44 FBKs were detected in the monocots *Os* and *Sb*. Forty-six and 71 FBKs were identified in the nonseed embryophytes *Sm* and *Pp* (Table I; Supplemental Table S1), which we subsequently refer to as lower land plants. Whereas animal model organisms and the single-celled green alga *Chlamydomonas reinhardtii* contain only a single FBK each (Supplemental Table S2), this subfamily of F-box genes has apparently dramatically expanded in land plants. The observation that FBKs are prevalent in high numbers not only in monocots and eudicots but also in the lower land plants indicates an early expansion of this F-box subfamily in land plant history.

The presence of the F-box and kelch domains for each of the proteins implemented in the following analyses was verified by the Pfam database (version 24.0, release October 2009; Sonnhammer et al., 1997). While we are not aware that FBKs for *Vv*, *Sb*, *Sm*, and *Pp* have been described before, we generally identified more FBKs than previously reported for the remaining

Table I. *Number of F-box kelch proteins in A. thaliana, V. vinifera, P. trichocarpa, O. sativa, S. bicolor, S. moellendorffii, and P. patens*

Species	No. of FBKs (K)	No. of F-Box Genes (F)[a]	No. of Protein-Coding Genes (G)[b]	Percent F/G[c]	Percent K/G[d]	Percent K/F[e]
A. thaliana	103	692	27,379	2.53	0.38	14.88
V. vinifera	36	156	30,434	0.51	0.12	23.08
P. trichocarpa	68	337	41,377	0.81	0.16	20.18
O. sativa	39	779	40,838	1.91	0.10	5.01
S. bicolor	44	549	34,496	1.59	0.13	8.01
S. moellendorffii	46	247	22,273	1.11	0.21	18.62
P. patens	71	165	39,727	0.42	0.18	43.03

[a]Number of F-box genes (*At, Os, Pt* [Xu et al., 2009]; *Vv* [Yang et al., 2008]; *Sb, Pp, Sm* [superfamily 1.73, release August 2010; Gough et al., 2001]). [b]Number of predicted protein-coding genes (*At* [TAIR9]; *Vv, Pt, Os, Sb, Sm, Pp* [Phytozome version 5.0]). [c]Percentage of genes that encode F-box proteins. [d]Percentage of genes that encode FBKs. [e]Percentage of F-box genes that contain kelch repeats.

three species. Initially, Gagné et al. (2002) identified 98 FBKs in *At*. We recovered all of these FBKs, but three of them (AT2G03460, AT2G29610, and AT4G39750) were not confirmed as FBK proteins by Pfam and therefore were excluded from further analysis. In addition to the remaining 95 genes/proteins identified by Gagné et al. (2002), we were able to identify eight novel FBKs. In *Pt* and *Os*, we recovered all previously published FBKs and were able to significantly increase these numbers (*Os*, 39 in this study versus 25 by Jain et al. [2007]; *Pt*, 68 in this study versus 40 by Xu et al. [2009]; Table I). Hence, the combination of BLASTP and HMM-based search algorithms efficiently identified previously known and numerous novel FBKs. Since the majority of the novel AtFBKs, for example, were present in the category "F-box proteins with unknown C-terminal domains" in the other studies, the better recognition of the kelch domain by our approach most likely contributes significantly to the identification of such novel FBKs. However, since the kelch motif is rather weakly conserved at the sequence level (Supplemental Fig. S1), the existence of additional yet undetected FBKs is likely. Furthermore, cases of complete loss of the kelch domain would not have been detected in this study. In contrast to plants, FBKs are absent from prokaryotes and occur only rarely in nonplant eukaryotic genomes, usually as single-copy genes with three conserved kelch repeats (Supplemental Table S2). This indicates a possible single common ancestor of *FBK*s in eukaryotes and a dramatic expansion in land plants. The ratio of genes encoding the F-box protein superfamily (F) and the FBK subfamily (K) relative to the whole protein-coding genome (G) is highest for *At* among the seven analyzed land plant species (F of G, approximately 2.5%; K of G, approximately 0.4%; Table I). However, due to the lower total number of F-box genes, the eudicots *Vv* and *Pt* show a higher ratio of FBK-encoding genes in relation to the total number of F-box genes (K of F, approximately 23.1% and approximately 20.2%, respectively). Since F-box proteins have been shown to be involved in numerous developmental processes (Lechner et al., 2006), one could expect lower land plants to reveal decreased numbers of F-box proteins relative to the complete genome. But this is obviously not the case, and interestingly, roughly half of the F-box proteins in *Pp* are FBKs (Table I).

FBKs and FBAs Are Closely Related

With both consensus sequence and HMM-based searches, numerous F-box proteins with so-called F-box associated domains were identified in addition to the FBKs (Table II; Supplemental Table S3). Despite its name, the F-box associated domain also occurs in the absence of the F-box domain (Jaso-Friedmann et al., 2002). Although FBKs and F-box proteins with C-terminal F-box associated domains (FBAs) are annotated as different F-box subfamilies in the Pfam database and previous publications (Xu et al., 2009), FBKs and FBAs are quite similar on the amino acid sequence level (Supplemental Fig. S2). Using our consensus sequences, we did not detect members of any F-box protein subfamily other than FBKs and FBAs. This indicates that the similarity is not due to the similarity of the F-box domain but rather to C-terminal regions of the proteins, most likely the similarity between the F-box associated domains and kelch repeats (Supplemental Fig. S2). Therefore, we speculate that the F-box associated domain might also form a tertiary propeller-like structure. Although FBAs represent the largest F-box protein subfamily, with 206 members in *At* (Xu et al., 2009), little functional information is available. So far, five AtFBAs have been characterized in detail and are involved in lateral root formation (Dong et al., 2006), pathogen responses (Kim and Delaney, 2002; Gou et al., 2009), and ethylene signaling (Qiao et al., 2009). Some additional FBAs are related to proteins that are part of the self-incompatibility system (Wang et al., 2004). It is unclear why this subfamily expanded to this extent in the self-fertile species *At*.

To get an insight into the phylogenetic relationship of FBKs and FBAs, we created phylogenetic trees including FBKs and FBAs of *At* and *Pp*, respectively (Fig. 1). For the *At* tree, we used the 103 FBKs that were confirmed by us and 206 FBAs, of which 193 were previously published (Xu et al., 2009). To construct the

Table II. *Number of F-box proteins with FBAs in A. thaliana, V. vinifera, P. trichocarpa, O. sativa, S. bicolor, S. moellendorffii, and P. patens*

Species	No. of FBAs	No. of F-Box Proteins with FBA and Kelch Domains	Previously Published Nos. of FBAs[a]
A. thaliana	205	1	193
V. vinifera	3	2	–
P. trichocarpa	47	4	32
O. sativa	38	1	2
S. bicolor	29	5	–
S. moellendorffii	2	1	–
P. patens	5	2	–

[a]Xu et al. (2009).

Pp tree, 71 FBKs and seven FBAs (five FBAs + two FBK/FBAs, both identified in this study) were used (Supplemental Tables S1 and S3). While the number of FBKs in *At* and *Pp* is rather similar in both species (103 in *At* versus 71 in *Pp*), the number of FBAs varies substantially (206 in *At* versus seven in *Pp*; Table II). Apparently, *FBA*s have dramatically expanded in *At*. Furthermore, in *At*, FBKs and FBAs form closely related but clearly distinct groups within the phylogenetic tree (Fig. 1). The same is true for *Pt*, *Vv*, *Os*, and *Sb* (Supplemental Fig. S3). In contrast to that, such an obvious phylogenetic distinction of FBKs and FBAs is not visible in the *Pp* tree (Fig. 1). In both *At* and *Pp*, the common ancestors of FBKs and FBAs contain kelch domains, indicating that FBKs may be evolutionary precursors of the FBAs. Taken together, our data indicate that kelch and F-box associated domains share a common evolutionary history.

Evolution of FBKs in Seven Land Plant Species

To compare FBKs in different land plant species, we created a phylogenetic tree including all identified FBKs of the seven analyzed species by using neighbor-joining (NJ) methods (Fig. 2A; Supplemental Fig. S4). Since previous studies generally analyzed the whole F-box protein superfamily, phylogenetic reconstructions were most feasible by using only the F-box domain. Analyzing F-box proteins with the same C-terminal interaction domains enabled us to include the amino acid sequence of the full-length proteins. Therefore, this tree reflects the evolution of both the F-box and kelch domains. Since we were unable to identify FBKs in Charophyceaes, a small group of predominantly freshwater green algae that represent the most recent common ancestor of land plants (Kenrick and Crane, 1997), we rooted the tree with the previously mentioned human FBK (Sun et al., 2009) and the only FBK that we identified in the annotated genome of the single-celled green alga *C. reinhardtii*. To confirm the NJ tree, three additional representative trees were constructed by using maximum likelihood, Bayesian, and NJ methods (Supplemental Figs. S5 and S6). The representative trees with the best likelihood support the NJ tree in Figure 2A (Supplemental Table S4). The significance of this finding

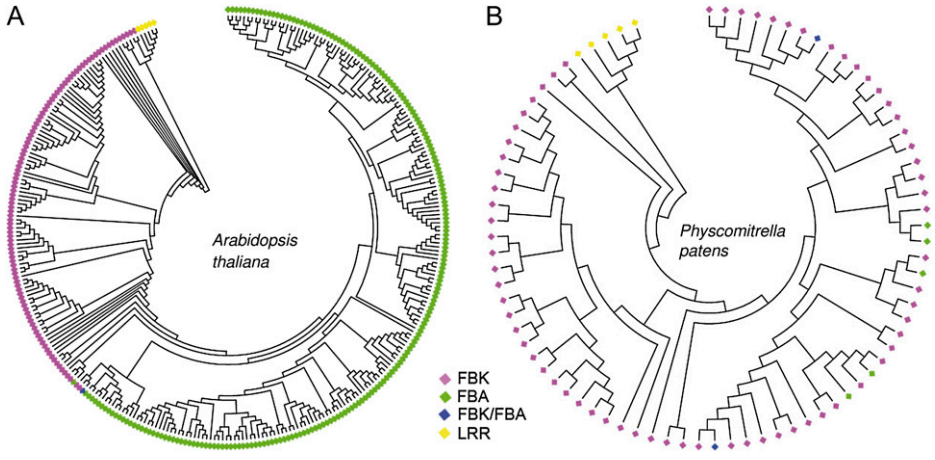

Figure 1. FBKs and FBAs are closely related to each other. A, NJ tree of 103 FBK proteins and 205 FBAs of *A. thaliana*. B, NJ tree of 71 FBKs and 5 FBAs of *P. patens*. Alignment of full-length protein sequences and construction of the NJ trees were performed in MEGA using a bootstrap value of 1,000. The *A. thaliana* tree was rooted with the auxin receptors (F-box LRRs) TIR1, AFB1, AFB2, AFB3, and AFB5. The *P. patens* tree was rooted with the respective homologous genes identified by BLASTP searches with AtTIR1. FBK/FBA proteins are characterized by overlapping positions of an F-box associated domain and individual kelch repeats.

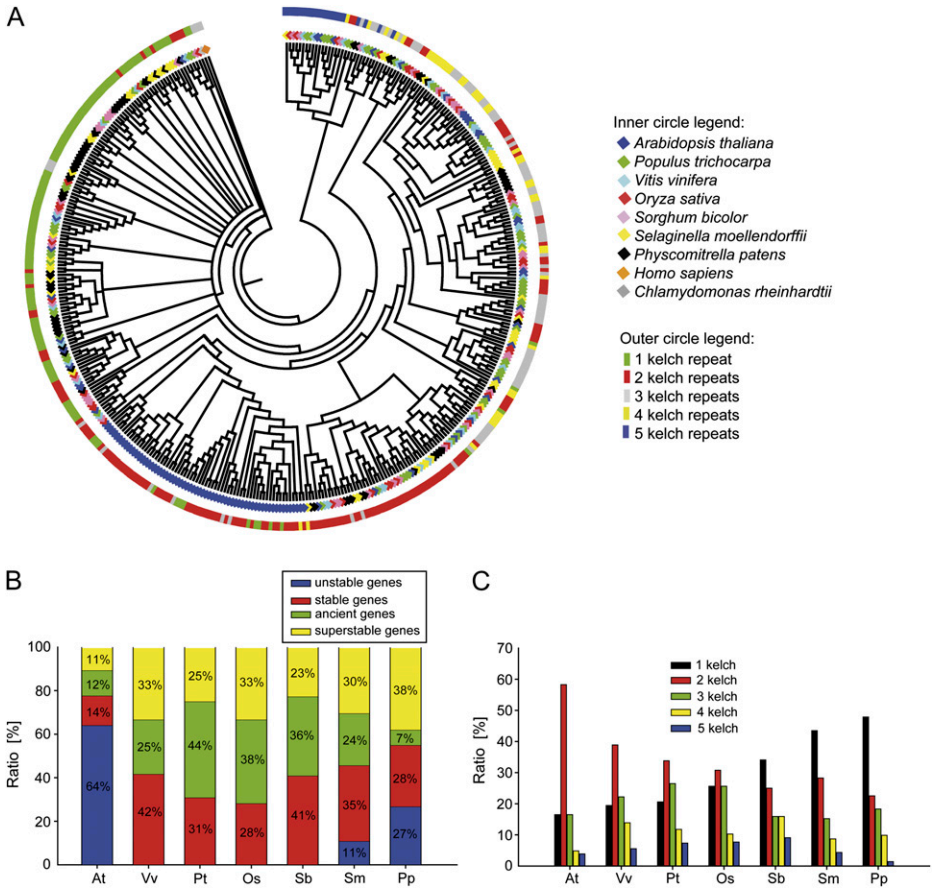

Figure 2. FBKs cluster according to their number of kelch repeats. A, NJ tree created with the full-length protein sequences of *A. thaliana*, *V. vinifera*, *P. trichocarpa*, *O. sativa*, *S. bicolor*, *S. moellendorffii*, and *P. patens* FBKs. The tree was rooted with FBKs of *C. reinhardtii* and *Homo sapiens*. The inner colored circle corresponds to the different species. The outer colored circle indicates the number of kelch repeats. B, Ratio of unstable, stable, ancient, and superstable FBKs in the seven analyzed land plant species. C, Ratio of FBKs with one, two, three, four, or five conserved kelch repeats according to Pfam in the seven analyzed land plant species.

was supported by comparing the topologies using p-SH (Shimodaira and Hasegawa, 1999) and 1sKH (Kishino and Hasegawa, 1989) tests. To further evaluate the quality of the NJ tree, we performed an exemplary search for orthologous genes using the 39 *Os* FBKs (Supplemental Table S1) as queries. The search was carried out in the ENSEMBL tool using the GRAMENE (http://www.gramene.org) and GEVO (http://synteny.cnr.berkeley.edu/CoGe) databases. Nearly all proteins annotated as orthologous in ENSEMBL also formed orthologous clusters in our NJ tree. Therefore, we conclude that the NJ tree topology accurately reflects the phylogenetic relations between FBKs in the analyzed species.

We identified a total of 40 well-supported clades ranging from species-specific clades to clades containing FBKs from all seven analyzed species. For the evolutionary classification of the genes in the all-species tree (Supplemental Fig. S4), we adopted the "stable/unstable" terminology coined by Thomas (2006) in a slightly modified manner and extended it with "superstable" and "ancient" categories (Supplemental Fig. S4). Unstable genes are lineage specific without clear orthologs in the other species analyzed. Stable genes are conserved across species with orthologs in at least one additional species. Superstable genes have orthologs in all analyzed species and, therefore, exhibit the highest degree of evolutionary conservation. It is conceivable that superstable genes perform functions in developmental or physiological processes conserved in all land plant species. The distinction between stable and superstable genes cannot be directly translated into the evolutionary age of a certain gene, because possible gene losses in individual species have to be taken into account. Therefore, we classified genes as ancient if they contain orthologs in at least one lower land plant, one monocot, and one eudicot species.

We identified eight clades of superstable genes (Supplemental Fig. S4). Depending on the species and the number of paralogs within a species, the ratio of genes in this category varies from 11% to 38% (Fig. 2B). While all species likewise contained various numbers of stable genes, we identified unstable genes only in *At* and the two lower land plant species (Fig. 2B; Supplemental Table S5). We are aware that the identification of unstable genes is strongly affected by the set of species included in the analysis. Since the two Poaceae species *Os* and *Sb*, for example, are closely related, the existence of unstable genes as we defined them is less likely than for species with no close relatives analyzed. However, if we account for this bias by screening for clades that contain either monocot-specific or *Pt-Vv*-specific FBKs, we find only three genes specific for *Os*

and *Sb* and none specific for *Pt* and *Vv*. Therefore, most *FBK*s in these species (*Pt*, *Vv*, *Os*, and *Sb*) likely perform functions conserved across species. In agreement with this, we find that the majority of *FBK*s in these species are of ancient origin (ancient + superstable; Fig. 2B). In *At*, on the other hand, we identified a large lineage-specific clade of unstable genes containing 64% of all *FBK*s in this species. This indicates that most *FBK*s in *At* result from lineage-specific duplication events. All unstable AtFBKs clustered in clade 22 (Supplemental Fig. S4). To assess how recent this clade evolved/expanded, we screened the genome of *Arabidopsis lyrata*, a close relative within the same genus, for orthologous genes. We identified *A. lyrata* orthologs for most of the *At* members of this clade (Supplemental Fig. S7), indicating that the expansion of this clade predates the split of *At* and *A. lyrata*. Furthermore, orthologs of this clade can also be identified in EST databases of other related Brassicaceae species (data not shown) suggesting that this clade originated after the separation of *Pt* and the Brassicaceae. Several of the *Sm* and *Pp FBK*s (20% and 25%, respectively) fell into clades containing only lower land plants (Supplemental Fig. S4). These genes either duplicated after the separation of lower land plants and angiosperms or were completely lost in the ancestor of monocots and eudicots. As in *At*, several *FBK*s of *Sm* and *Pp* (11% and 27%) are lineage specific (Fig. 2B). Taken together, while most eudicots and both monocots contain only FBKs that are conserved across species, significant portions of *At* and lower land plant FBKs are lineage specific/unstable.

We next estimated the number of *FBK*s in the most recent common ancestor (MRCA) of the seven species analyzed in this study and determined the number of gained and lost genes. Reconciliation of the all-species tree identified 40 clades containing orthologous genes that were present in the potential MRCAs of the seven analyzed species (N1; Fig. 3). Furthermore, we identified 37 orthologous genes in the lower land plant MRCA (N2), the angiosperm MRCA (N3), and the monocot MRCA (N4) and 38 in the MRCA of eudicots (N5). When we compared the number of ancestral genes with those in the extant species, it appeared that the *FBK* family has expanded in several of the analyzed species. In *At*, for example, the number of *FBK*s increased approximately 2.5-fold since the divergence of the various eudicot species from their respective MRCA. This is consistent with the situation of the whole F-box superfamily in *At*, which has increased in size as much as 3-fold since the divergence of eudicots and monocots 145 million years ago (Xu et al., 2009). In *Vv* and *Os*, the number of *FBK*s remained largely unchanged since the emergence of angiosperms and the divergence of eudicots and monocots, respectively. In summary, while *C. reinhardtii* and animal species usually contain a single-copy *FBK* (Supplemental Table S2), the number of *FBK*s increased dramatically in land plants (N0–N1; Fig. 3). The number of *FBK*s then remained relatively stable

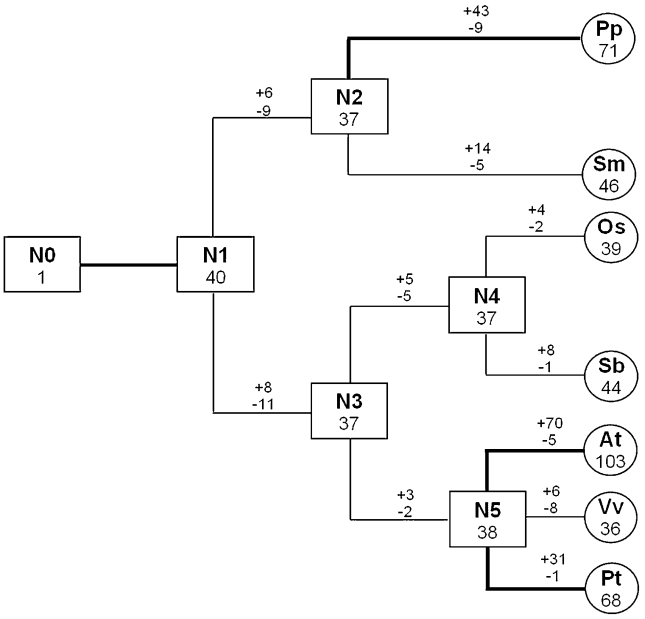

Figure 3. Evolutionary change in the number of FBK proteins in land plants. The numbers in squares and circles represent the maximum numbers of genes in ancestral and extant species, respectively. The numbers with plus and minus indicate the gene gains and losses, respectively, for each branch. Thick lines represent branches with high gene expansion rate. N0, Eukaryotic ancestor; N1, land plant ancestor; N2, lower land plant ancestor; N3, angiosperm ancestor; N4, monocot ancestor; N5, eudicot ancestor. Branch lengths are not in proportion to evolutionary time.

through evolutionary history from the land plant MRCA (N1) to the MRCAs of the lower land plants (N2) and monocots/eudicots (N4/N5; Fig. 3). Only after the separation of the various eudicot species did *FBK*s once more expand significantly. Such inconsistent rates of gene gains over time had previously been demonstrated by Hanada et al. (2008), who showed that gain rates for branches linked together by older ancestral nodes are smaller than those linked by younger branches.

FBKs Cluster According to Their Number of Kelch Repeats

The all-species tree shows that FBK proteins cluster according to the number of kelch repeats (Fig. 2A, outer circle). In principle, the tree shows large clades including mainly FBKs with one and two kelch repeats. FBKs with higher numbers of kelch repeats are most common in an additional clade, whereby the FBKs with five kelch repeats are clearly concentrated in a distinct subclade. As the consensus sequences (Supplemental Fig. S1) indicated, kelch repeats may be more similar when found at the same position in different proteins compared with repeats within the same protein. To substantiate this observation, we performed a permutation test to estimate whether the similarity of kelch

repeats within a protein differs from the similarity between proteins. And indeed, kelch repeats at the same position between proteins are significantly more similar to each other than the repeats within the same protein ($P = 2 \times 10^{-6}$; Supplemental Fig. S8). This indicates that multiple kelch repeats did not arise independently in each protein but were already present in "the" ancestral FBK. In numerous proteins, we detected conserved amino acid residues downstream of the last Pfam-confirmed kelch repeats that were quite similar to a kelch motif structure but not conserved well enough to be considered a kelch motif by Pfam. We assume that these conserved regions are rudimentary kelch repeats that decayed over time. The only FBK we identified in *C. reinhardtii* contains three kelch repeats. Likewise, the FBKs identified in other animal model species also contain three conserved kelch repeats recognized by Pfam (Supplemental Table S2). Hence, we hypothesize that the MRCA of eukaryotic FBKs was formed by the combination of an F-box and three conserved kelch repeats.

Unstable *FBK*s Are Organized in Clusters of Tandem Repeats

The hypothesis that correlates stable/superstable FBKs with conserved and potentially ancient functions in plant development and physiology likewise suggests that unstable genes constantly continue to evolve by birth-death evolution (Thomas, 2006). Since significant portions of F-box genes are arranged in tandem repeats, this hypothesis would predict that such tandemly arranged genes are primarily unstable genes. Indeed, this prediction is supported by the chromosomal localization of *FBK*s in *At* (Fig. 4), the species with the highest ratio of unstable genes (64%; Fig. 2B). Unstable genes are strongly clustered, while stable and superstable genes are evenly scattered over the chromosomes (Fig. 4). Substantiating this, the majority of unstable genes in *At* (62%) emerged after the most recent whole genome duplication event (Blanc et al., 2003; Bowers et al., 2003; http://wolfe.gen.tcd.i.e./athal/dup). In contrast to *At*, where 35% of the *FBK*s are arranged in tandem repeats, considerably fewer *FBK*s are arranged in tandem repeats in *Pt* (3%), *Vv* (17%), *Os* (5%), and *Sb* (14%), indicating that in these species, *FBK*s mainly emerged by mechanisms other than tandem duplication. Analysis of the *Pt* genome, for example, revealed evidence of a recent whole genome duplication event (8–13 million years ago) that affected approximately 92% of the *Pt* genome (Sterck et al., 2005; Tuskan et al., 2006). In agreement with the low ratio of tandem repeat *FBK*s in *Pt*, *Vv*, *Os*, and *Sb*, they do not contain unstable genes (Fig. 2B). Furthermore, with the exception of *Pt*, the total number of *FBK*s in these species is rather similar to that of the respective MRCAs (Fig. 3). In summary, our results suggest that after the dramatic expansion of the *FBK* gene family in land plants that followed the divergence from *C. reinhardtii*/single-celled green algae, a second wave of expansion can largely be explained by tandem duplications.

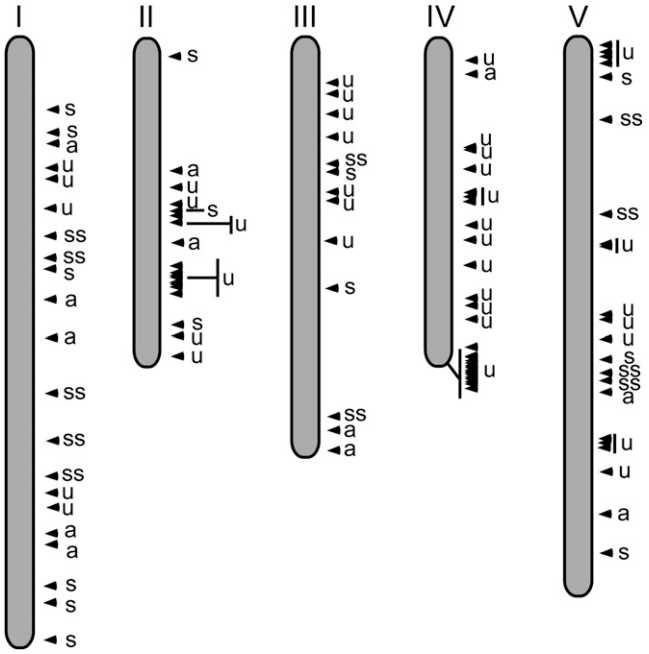

Figure 4. Chromosomal distribution of *A. thaliana FBK*s. Approximate positions of *FBK*s are displayed on the respective chromosome (black triangles). Letters denote evolutionary classification of *FBK*s according to Supplemental Figure S4. a, Ancient; s, stable; ss, superstable; u, unstable.

Superstable and Unstable FBKs Carry Different Signatures of Selection

If stable and superstable genes have evolved to recognize similar targets across species, one would expect purifying selection to act on such genes. Genes that confer adaptational properties, on the other hand, typically are under positive selective pressure. To examine whether these expectations also hold for *FBK*s, we determined K_a/K_s ratios for superstable and unstable genes of *At*. For the calculation of K_a/K_s ratios, we first identified the closest orthologs for each gene in the genome of the close relative *A. lyrata* (Supplemental Fig. S7) and included only those *At* genes that had a single ortholog in *A. lyrata*. K_a/K_s ratios of 0.16 for the complete coding regions for superstable *FBK*s (Fig. 5A) strongly indicate purifying selective pressures. In contrast to that, unstable genes seem to be more close to neutral selection, as inferred by significantly higher K_a/K_s ratios (0.72; $P < 0.0001$) for the complete coding region (Fig. 5A).

We then randomly selected representative genes for sliding window analysis to identify possible differences between F-box and Kelch domains (Fig. 5, B and C). For unstable genes, sliding window analysis clearly shows numerous sites/regions under positive selection, with $K_a/K_s >> 1$ (Fig. 5C). Furthermore, for unstable genes, we observed that the F-box domain had generally lower

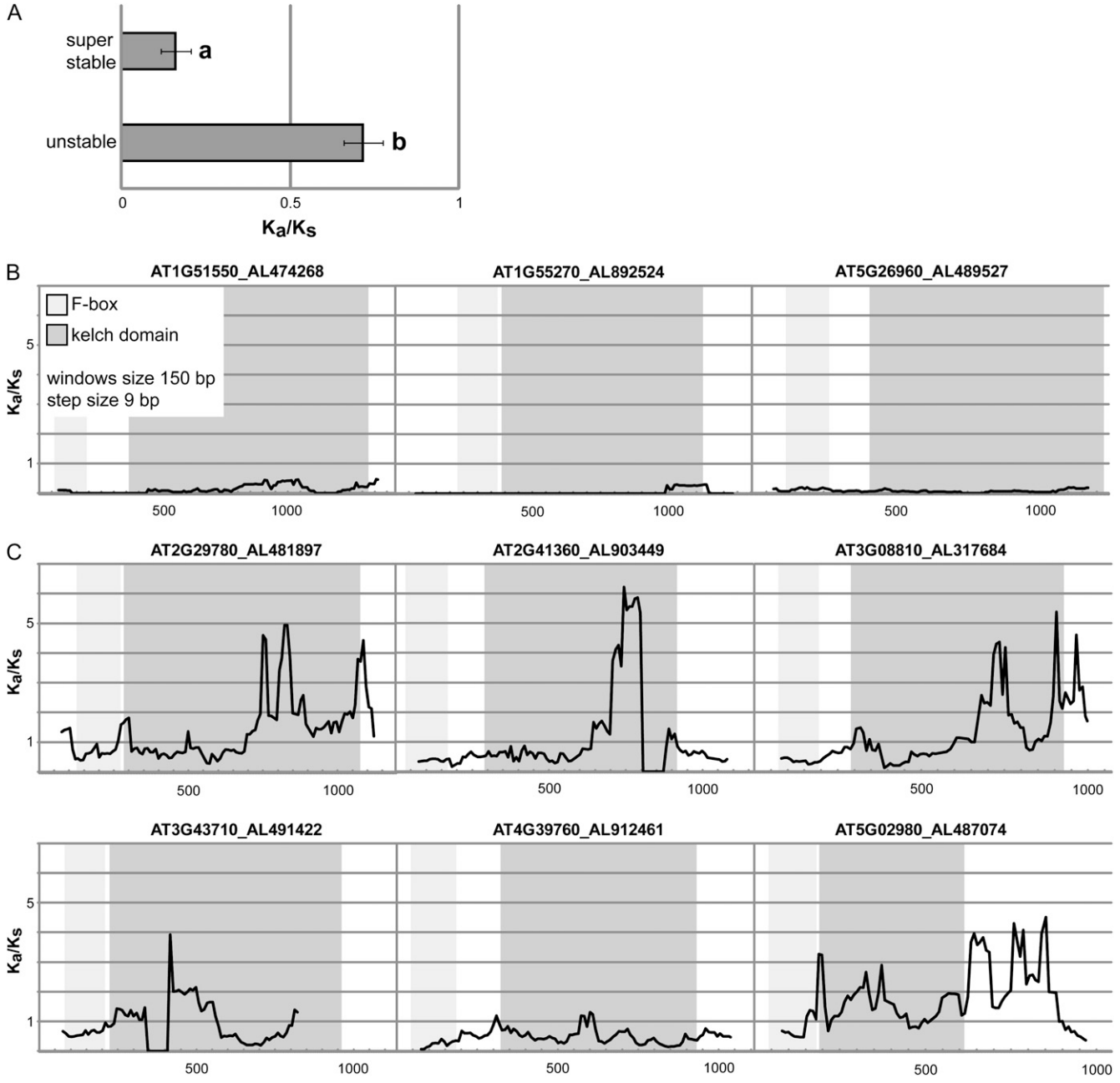

Figure 5. Divergence levels of *FBK*s (*A. thaliana* versus *A. lyrata*). A, Mean K_a/K_s ratios of superstable ($n = 10$) and unstable ($n = 37$) FBKs. Only *A. thaliana* genes with a single *A. lyrata* ortholog were included (Supplemental Fig. S7). Error bars denote SE. a and b denote significant differences according to Student's *t* test ($P < 0.0001$). B, Sliding window plots of representative superstable *FBK*s. C, Sliding window plots of representative unstable *FBK*s. For sliding window analysis, nucleotide sequences of *A. thaliana* (indicated by Arabidopsis Genome Initiative identifier) and homologous nucleotide sequences of *A. lyrata* (indicated by protein identifier according to the Joint Genome Institute) were used. Window size was 150 bp, and step size was 9 bp. For *A. lyrata* protein 491422, only a partial coding sequence could be analyzed. Light gray boxes highlight the F-box domain, and dark gray boxes highlight the kelch domain positions.

K_a/K_s values in comparison with the C-terminal part of the proteins/genes including the kelch domain (Fig. 5C). This suggests that as a consequence of natural selection, ASK-binding patterns remain conserved while the target-recruiting kelch domain has evolved to recognize new target proteins.

Closely Related *FBK*s Are Differentially Expressed in *At*

The recent expansion of *FBK*s especially in *At* raises two interesting questions. First, are unstable genes generally expressed, or have many of them already become pseudogenes? Second, are phylogenetically

closely related *FBK*s functionally redundant, or have duplicated genes subfunctionalized? To address these questions, we made use of the publicly available AtGenExpress data (Schmid et al., 2005; Toufighi et al., 2005) and additionally selected a small clade consisting of seven closely related AtFBKs (clade A in Fig. 6B) for further molecular characterization.

Although both stable (including also ancient and superstable) and unstable genes were expressed at rather low levels in the AtGenExpress extended tissue series (Schmid et al., 2005), the average expression levels across tissues were significantly higher for stable than for unstable genes ($P < 0.001$; Fig. 6A). Fifty-eight percent (26 of 45 that were present on the ATH1 array) of the unstable genes had mean absolute expression levels of less than 25 across the 86 tissues/developmental stages assessed (Supplemental Data Set S1). However, only four of these 26 had absolute expression levels of less than 50 for all tissues/developmental stages assessed, demonstrating that the vast majority of these unstable *FBK*s were significantly higher expressed (greater than 50) in at least a few selected tissues/developmental stages (Supplemental Data Set S1). This indicates temporal and/or spatial specialization of unstable genes, which argues against widespread pseudogenization.

To investigate possible functional diversity of AtFBKs in general, we again used the AtGenExpress data. Both members of phylogenetically closely related unstable FBKs organized in tandem repeats (e.g. clades B + C in Fig. 6B) and clades of stable FBKs (clade A in Fig. 6B) grouped into different clades when clustered according to their coexpression profiles (Fig. 6C). These array data could be confirmed by quantitative PCR data of the seven clade A genes (Supplemental Fig. S9). Together with the above-described temporal and/or spatial specialization of unstable genes, this indicates that *FBK*s within a common phylogenetic clade can be differentially regulated at the mRNA level and therefore could have evolved different functions or spatiotemporal specificities.

Posttranslational mechanisms that might create functional diversity between family members are subcellular localization and the ASK-binding patterns that define the specific SCF complexes in which a certain F-box protein may be incorporated. Subcellular localization was examined with GFP-FBK fusion proteins of the seven clade A FBKs (Fig. 6B), which were transiently transformed into epidermal cells of *Nicotiana benthamiana* (Fig. 7, A–H). Six of them localized exclusively to the nucleus. AT5G40680 was additionally located in the cytoplasm. In agreement with this, the 26S proteasome is present in both the cytoplasm and the nucleus (Book et al., 2009). The specific interaction of the FBKs with 17 of the 21 ASK adaptor proteins was examined in the yeast two-hybrid system. ASK6 and ASK15 were excluded from the interaction studies because they were shown to be pseudogenes (Seki et al., 2002; Takahashi et al., 2004). ASK12 and ASK18 were excluded because they showed autoactivity in our system. Figure 7I indicates that the ASK-binding pattern seems to be rather unspecific for the seven selected FBKs. Similar unspecific binding had been reported previously for other F-box proteins such as the kelch domain-containing ZTL (Risseeuw et al., 2003). The seven analyzed FBKs interacted with 11 to 17 of the tested ASK proteins. However, a pattern is visible in which AT1G26930, AT3G27150, AT5G60570, and AT5G40680 interact with nearly the same ASK proteins. The same is true for AT2G02870, AT1G74510, and AT1G14330. Taken together, while the selected FBKs showed rather similar ASK interaction patterns and subcellular localizations, they differed considerably in their expression profiles, indicating that possible functional diversification may be achieved by a combination of transcriptional regulation and positive selection acting on the kelch domain.

DISCUSSION

Comparison of gene family content across species may provide insight into evolutionary mechanisms that have shaped adaptation and diversity (Rubin et al., 2000). The F-box gene superfamily represents one of the largest and fastest evolving gene families in the plant kingdom (Clark et al., 2007). While this superfamily in its entirety had previously been characterized on a phylogenetic and evolutionary scale (Gagné et al., 2002; Yang et al., 2008; Xu et al., 2009), a detailed characterization of one of its subfamilies allows us to turn the focus from the F-box domain to a specific protein-protein interaction domain. The F-box protein subfamily we chose for this study was composed of an N-terminal F-box with various numbers of C-terminal kelch repeats.

The Kelch Repeat Domain

In yeast, *Drosophila*, and mammalian F-box proteins, WD40 repeats and LRRs are the predominant substrate recruitment domains (Skaar et al., 2009a, 2009b). Interestingly, both kelch and WD40 repeats adopt the stereotypical topology of a β-propeller. As kelch and WD40 repeats have no similarity at the sequence level, it was speculated that convergent evolution of a subset of F-box proteins has originated a common tertiary structure specialized in protein-protein interactions (Andrade et al., 2001).

Kelch repeat proteins have become widespread in evolution. Typically, five to seven kelch repeats form a β-propeller with the blades arranged around a central axis. Intrablade and interblade loops of varying lengths protrude above, below, or at the sides of the β-sheets and contribute variability to the binding properties of individual β-propellers (Fülöp and Jones, 1999; Jawad and Paoli, 2002; Prag and Adams, 2003). The entire kelch β-propeller forms a functional unit that can be found in combination with other conserved protein domains (Adams et al., 2000). In plants, kelch motifs

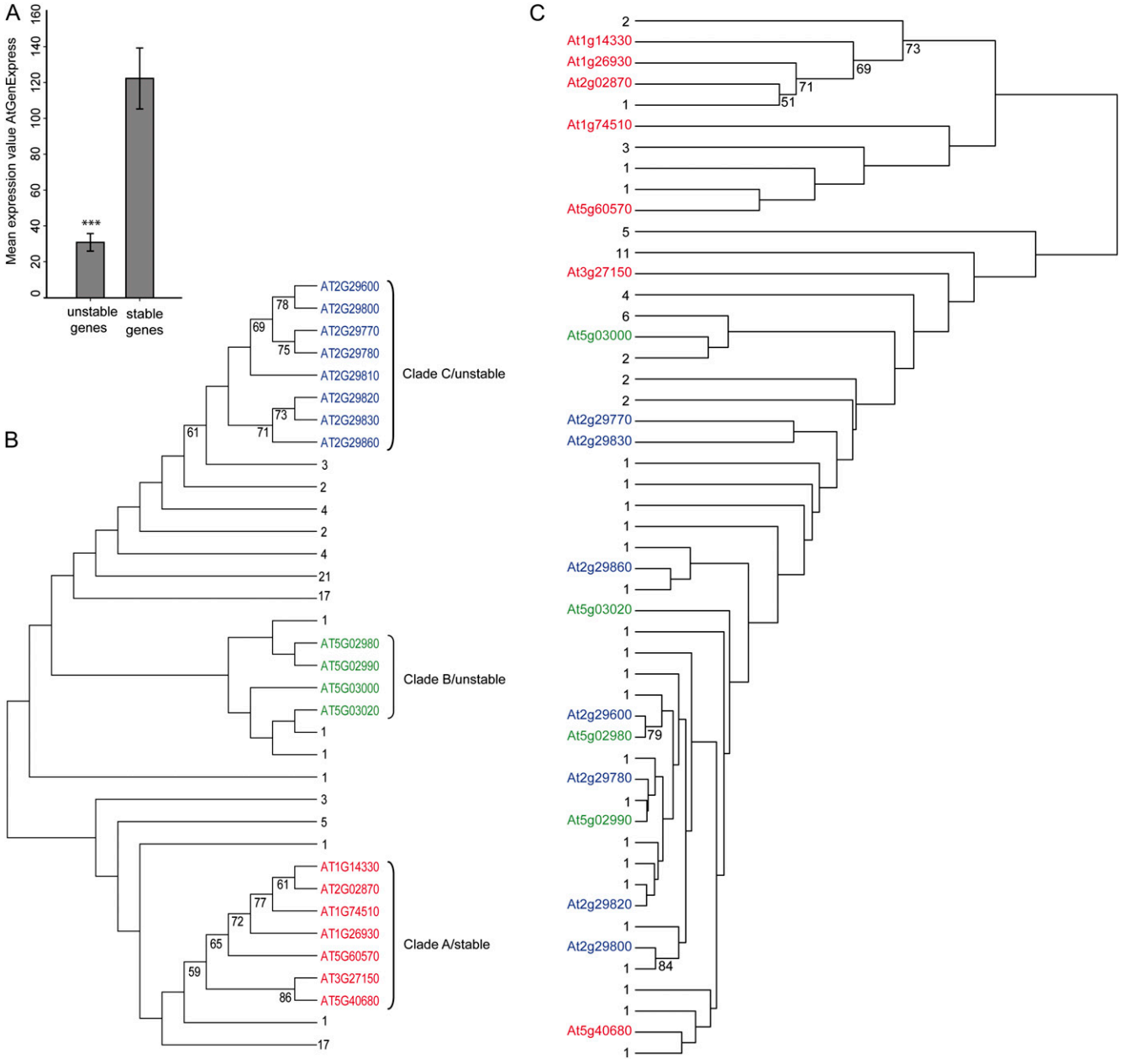

Figure 6. Differential transcription profiles of phylogenetically closely related *FBK*s. A, Mean expression values for stable (including ancient and superstable) and unstable *A. thaliana FBK*s extracted from the AtGenExpress_Plus extended tissue series (Schmid et al., 2005). Error bars represent SE. Statistical significance was assessed using Student's *t* test (*** $P < 0.001$). B, NJ tree of 103 *A. thaliana* FBKs based on amino acid sequence homology. C, Phylogeny based on coexpression data from the AtGenExpress_Plus extended tissue series including 81 FBKs of *A. thaliana*. Discrepancy in the number of *FBK*s between the trees results from 22 missing *FBK*s on the ATH1 microarray. Noninformative clades were collapsed and labeled according to the number of underlying *FBK*s. Numbers at nodes display bootstrap values greater than 50%. Classification of clades as stable and unstable is according to the categorization of *FBK*s in Supplemental Figure S4.

have been identified in proteins without additional conserved domains (Prag and Adams, 2003) as well as in combination with various other N- and/or C-terminal domains, such as C-terminal phosphatase domains (Mora-García et al., 2004) or N-terminal acyl-CoA-binding domains (Suzui et al., 2006; Du et al., 2010). However, the combination with N-terminal F-box domains seems to be most prevalent. With the exception of AtAFR (AT2G24540), all functionally characterized kelch proteins in plants contain a minimum of five kelch repeats. Therefore, they match the prerequisites to form a closed propeller structure with stabilized interactions between the first and last blades. We found, however, that the vast majority of FBKs in plants con-

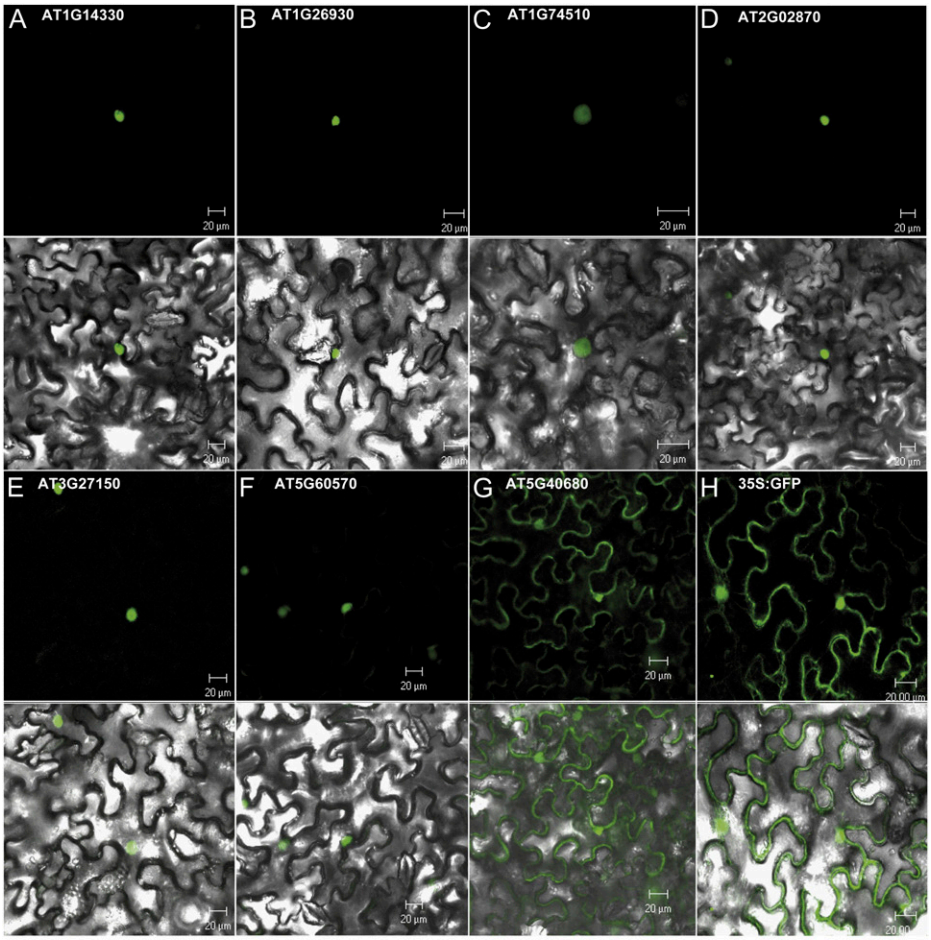

I

	AT1G14330	AT1G26930	AT1G74510	AT2G02870	AT3G27150	AT5G40680	AT5G60570
ASK1	■		■	■			
ASK2	■		■	■			
ASK3	■	■	■	■	■		■
ASK4	■	■	■		■	■	■
ASK5	■	■	■	■	■	■	■
ASK7	■	■	■	■	■	■	■
ASK8	■	■	■	■	■	■	■
ASK9	■		■	■			
ASK10	■	■	■	■	■	■	■
ASK11	■		■	■			
ASK13	■	■	■	■	■	■	■
ASK14	■		■	■			
ASK16	■	■	■	■	■	■	■
ASK17	■	■	■	■	■	■	■
ASK19	■	■	■	■	■	■	■
ASK20	■	■	■	■	■	■	■
ASK21	■	■	■	■	■	■	■
LaminC							

Figure 7. Protein features of selected *A. thaliana* FBKs. A to H, Subcellular localization of 35S::GFP-FBK constructs in leaf epidermal cells of *N. benthamiana*. I, Yeast two-hybrid analysis of specific interactions of the selected FBK proteins with ASK adaptor proteins. BD fusions of ASK proteins were tested with AD fusions of FBK proteins. Gray and white boxes indicate positive and negative interactions, respectively. Human LaminC served as a negative control.

tain less than three kelch repeats (Fig. 2C). It is questionable, therefore, whether functional β-propellers can be formed in such proteins. A survey of the Pfam database for kelch motif-containing proteins revealed a total of approximately 400 different protein architectures (irrespective of the species background and the presence of other functional domains). Approximately 65% of the proteins underlying these architectures contain only one or two kelch repeats. Since it is unlikely that this majority of kelch domains is nonfunctional, several scenarios are possible. (1) It is conceivable that FBK proteins with fewer kelch repeats dimerize to achieve a full set of propeller blades. (2) Or they operate via a completely different mechanism to interact with target proteins. (3) Alternatively, a significant number of these genes may be nonfunctional and represent the remains of once functional *FBK*s. (4) Lastly, because of poor sequence conservation of the kelch motif, the missing repeats are present but not recognized by Pfam. In agreement with the latter notion, we detected

conserved C-terminal residues that resemble the kelch motif structure. Furthermore, other motif recognition algorithms/databases such as Interpro recognize a complete kelch β-propeller motif (IPR015915) in the majority of the FBKs. Hence, we assume that most plant FBKs do indeed form functional β-propeller-like tertiary structures. Such conserved C-terminal residues indicate gradual degeneration of the kelch consensus sequence toward the C terminus. In contrast to earlier studies from *Drosophila* (Xue and Cooley, 1993; Bork and Doolittle, 1994), we found that kelch motifs at given positions within the kelch repeat domain between proteins are more similar to each other than different kelch motifs within a protein (Supplemental Fig. S8). In agreement with this, we derived specific consensus sequences for each repeat position (Supplemental Fig. S1), and FBK proteins in the all-species tree generally clustered according to their number of kelch repeats (Fig. 2A). This may simply reflect the progressive degeneration of the C-terminal kelch repeat primary sequence or, alternatively, may indicate that each blade position in the β-propeller may require specific functional residues.

The All-Species Tree Identifies Superstable, Stable, and Unstable Genes

The all-species tree contains valuable information on several levels. It reveals the phylogenetic architecture of FBKs between species and identifies clades with genes conserved across species as well as lineage-specific clades. In a similar approach, Thomas (2006) performed a detailed characterization of F-box proteins in three *Caenorhabditis* species. The author divided the genes into stable and unstable categories. It was hypothesized that stable genes most likely became devoted to specific endogenous substrates long ago, while unstable genes continued to evolve by birth-death evolution and are primarily involved in recognizing foreign proteins and targeting them for degradation (Thomas, 2006). Accordingly, he found strong evidence for positive selection in the C-terminal substrate-binding domains of unstable genes, while those of stable genes seemed to be under purifying selection. In this study, we adopted similar gene categories and identified similar signatures of natural selection acting on *FBK*s in *At*. While superstable *FBK*s had very low K_a/K_s values, indicating purifying selective pressures, K_a/K_s ratios of unstable *FBK*s were significantly higher (Fig. 5A). Sliding window analyses showed that numerous regions in the unstable genes seemed to be under strong positive selection (Fig. 5C). While in most cases the F-box domain is rather conserved, it is the substrate-recruiting kelch domain that seems to be positively selected for. Hence, a picture emerges in which kelch repeats evolve in a manner that supports the constant development of novel substrate specificities. Furthermore, as predicted, we found unstable *FBK*s from *At* to be strongly clustered with respect to their chromosomal localization.

If this large pool of unstable *FBK*s in *At* is indeed used to recruit targets for specialized environmental responses with potential adaptive importance, it is clear why to date only a tiny fraction of members of the plant F-box gene superfamily have been identified in forward genetic screens, which are usually designed to identify components of more general mechanisms of development or physiology. Consequently, the few biologically characterized FBKs are, as expected, ancient genes with conserved functions. AFR, ZTL, FKF1, and LKP2 are all members of phylogenetic clades with orthologs in several species (Supplemental Fig. S4) and perform functions in essential physiological processes such as the regulation of light responses and circadian rhythms. And, not surprisingly, all but one of the 38 F-box genes functionally characterized to date in *At* have orthologs in one or several other of the species analyzed in this study (data not shown). The only exception is SUPPRESSOR OF NIM1-1 (SON1; Kim and Delaney, 2002). The substrate/target protein of SON1 is not known. But remarkably, SON1 plays a role in pathogen response and therefore perfectly fits Thomas' (2006) category of unstable genes with a possible function in the recognition of foreign proteins. While unstable genes are dominating in *At*, we identified significantly fewer or no unstable *FBK*s at all in the other species analyzed in this study. Following the initial hypothesis, the vast majority of FBKs in these species most likely perform conserved functions. In agreement with this, more than 50% of *Vv*, *Pt*, *Os*, *Sb*, and *Sm* FBKs fall into the ancient or superstable category (Fig. 2B). Therefore, at least for *FBK*s, the emerging paradigm of rapidly evolving gene families organized in tandem repeats cannot be easily transferred from *At* to other plant species.

Functional Redundancy and Subfunctionalization

The total number of *FBK*s among the plant genomes assessed in this study was highest for *At*, which made this species a suitable model to study possible functional consequences of gene family expansion. Although Gagné et al. (2002) argued that direct sequence alignments between members of the same clade suggested that most of the *At* F-box proteins do not have obvious functional paralogs, molecular characterization of numerous F-box proteins has meanwhile demonstrated the opposite. At least partial functional redundancy could be shown for the auxin receptors (Dharmasiri et al., 2005), the ethylene signaling components EIN3-BINDING F-BOX PROTEIN1/2 (An et al., 2010) and EIN2-TARGETING PROTEIN1/2 (Qiao et al., 2009), VIER F-BOX PROTEINE1 to VIER F-BOX PROTEINE4, which are involved in root development (Schwager et al., 2007), and also for the FBKs ZTL, FKF1, and LKP2 (Baudry et al., 2010). Hence, although we have no functional information on the vast majority of *FBK*s, rapid gene family expansion suggests scenarios wherein natural selection favors additional copies either for increased dosage or an increased

arsenal of molecular weaponry via subfunctionalization (Demuth and Hahn, 2009). Our expression analysis of *AtFBK*s supports the latter and clearly shows differences in transcriptional regulation within phylogenetic subclades. We found similar patterns for subclades with both genetically unlinked members and those that are organized in tandem repeats (Fig. 6, B and C). Hence, the transcriptional divergence seems to be independent of the genetic mechanism that led to the increase in copy numbers. Similar transcriptional and posttranscriptional diversification (by microRNAs) could be shown by GUS-reporter assays for the auxin receptors, members of the F-box LRR subfamily (Dharmasiri et al., 2005; Parry et al., 2009), suggesting that differential expression indeed contributes to functional diversification. Furthermore, although unstable genes had significantly lower mean expression values across a large number of tissues (Fig. 6A), this is most likely due to the specialization of spatiotemporal expression patterns. While the higher expressed stable genes had significant expression values in many tissues, the expression of unstable genes was specific for few selected tissues and/or developmental stages (Supplemental Data Set S1), again arguing that duplicates here subfunctionalized.

On the other hand, our molecular characterization of a selected subclade containing seven FBKs revealed conservation of protein features such as subcellular localization and ASK-binding patterns. This indicates that the family members are generally able to integrate into the same SCF complexes and act in the same cellular compartments. Therefore, we hypothesize that after copy number expansion, two genetic mechanisms mainly contributed to potential subfunctionalization of FBK family members in *At*: (1) different transcriptional regulation, and (2) positive selection acting primarily on the kelch domain of unstable *FBK*s, likely resulting in modified substrate specificities.

CONCLUSION

F-box proteins with C-terminal kelch repeats are classic multidomain proteins. While the F-box connects the protein via a restricted set of ASK adaptor proteins to the rest of the SCF complex, the C-terminal domains most likely recruit target proteins destined for proteasomal degradation. The diversity of potential substrates is mirrored by the number of different interaction domains C terminal to the F-box with kelch repeats being widespread in land plant genomes. Although there is hardly any experimental evidence addressing the function of the vast majority of these genes, their patterns of evolution are strongly suggestive. All species analyzed in this study contained numerous stable and superstable *FBK* genes, which are under purifying selection and potentially perform conserved functions in land plant development and physiology. Depending on the species background, several clades dramatically expanded in a lineage-specific manner. These clades contain genes that most likely evolved (or still evolve) to perform functions specific for the respective lineage. They may contribute to adaptational processes, as signatures of positive selection suggest.

Evolutionary and phylogenetic analyses of F-box protein subfamilies with other C-terminal domains (e.g. LRR, F-box associated domain) are desired to enable direct comparisons with our findings for the FBK subfamily. We hypothesize that detailed analyses of additional subfamilies with a focus on the evolutionary categories (stable/unstable) and selective pressures may reveal subfamily-specific patterns. Certain subfamilies with characteristic protein-protein interaction domains may be more capable to generate novel functions that could confer selective advantages and therefore drive adaptational processes. Naturally, subfamilies with large portions of unstable genes would be candidates for this category. Other subfamilies may contain predominantly stable or superstable genes and perform primarily conserved functions across species. However, the assignment of specific subfamilies to either category may be species dependent, as this study shows for F-box proteins with C-terminal kelch repeat domains. Additional insight will be gathered by molecular population genetic analyses primarily in *At* that will become feasible in the near future through the 1,001 Genomes Project (Weigel and Mott, 2009). Lastly, this analysis should provide a good basis to select promising candidates for reverse genetic characterization of *FBK*s.

MATERIALS AND METHODS

Identification of FBKs in Different Land Plant Genomes

The most recent annotated version of cDNAs and proteins from each of the genomes was downloaded from the respective genome sequence sites (status March 2009: *Arabidopsis thaliana* from The Arabidopsis Information Resource [ftp://ftp.arabidopsis.org/home/tair, arabi_cds_v.090704]; *Populus trichocarpa* [version 1.1], *Physcomitrella patens* [version 1.1], and *Selaginella moellendorffii* [filtered model 3] from the Joint Genome Institute [http://www.jgi.doe.gov/]; *Vitis vinifera* [version 1] from Genoscope [http://www.cns.fr/externe/GenomeBrowser/Vitis/]; *Oryza sativa* [Osjaponica_cds300503] from The Rice Genome Annotation Project [ftp://ftp.plantbiology.msu.edu/pub/data/Eukaryotic_Projects/o_sativa/annotation_dbs]; *Sorghum bicolor* [version 1.4] from the Munich Information Center for Protein Sequences [http://mips.helmholtz-muenchen.de/plant/sorghum]). Published FBK protein sequences (Gagné et al., 2002; Yang et al., 2008; Xu et al., 2009) were used as first queries for FBKs using BLASTP and TBLASTN (Altschul et al., 1997). Identified full-length cDNAs were translated in the correct frame. Putative FBK sequences were aligned using ClustalX (Thompson et al., 2002). Alignments were verified manually, and a consensus sequence was created for each of the motifs of interest with the help of the Weblogo software package (http://weblogo.berkeley.edu/logo.cgi). Consensus sequences were then used in a BLASTP search to identify more FBKs from the downloaded genomes. This alignment was used to generate an HMM model using the program hmmbuild from the HMMER program suite (Eddy, 1998). The HMM model was further improved by calculating HMM parameters with the hmmcalibrate package (Eddy, 1998). Using hmmsearch, the HMM model was applied in a search against the most recent protein annotations from each plant. To confirm the presence of both F-box and kelch domains in the obtained sequences ($e < 3.8$), we further compared the results from hmmsearch and the Pfam databases (Sonnhammer et al., 1997) with the hmmpfam package. Our domains of interest are annotated in Pfam as PF00646 (F-box), PF01344 (kelch domain 1), PF07646 (kelch domain 2), PF04300 (FBA_1), and PF08268 (FBA_3).

We did not use the domain DUF1668 (PF07893), classified as a member of the kelch family in Pfam, because this domain was not detected in our searches.

Construction of F-Box and Kelch Consensus Sequences

To construct consensus sequences of the F-box and kelch 1 repeat, complete protein sequences of FBKs of all seven plant species were aligned using ClustalW (Thompson et al., 2002) and corrected manually. To create consensus sequences of the kelch 2, kelch 3, kelch 4, and kelch 5 repeats, only FBKs were aligned that actually include the required number of kelch repeats. Gaps occurring in the alignment were deleted if more than 75% of the aligned sequences contained a gap in the same position. Positions of F-box and kelch domains were predicted according to the matches in Pfam (Sonnhammer et al., 1997).

Alignments of Kelch Repeats and Phylogenetic Reconstruction

With the hmmalign package from the HMMER suite, alignments for the phylogenetic reconstruction were created by applying the HMM-calibrated model obtained previously. All 407 FBKs and the outgroup protein sequences aligned with hmmalign were used to generate a final tree constructed with the NJ algorithm implemented in PHYLIP (bootstrap = 100, seqboot; Felsenstein, 1989). To confirm the robustness of the NJ tree, we built trees using at least one representative sequence of each of the defined clades in the NJ tree and built phylogenies using two additional methods: maximum likelihood (PHYLIP; bootstrap = 100, amino acid substitution model, Jones-Taylor-Thornton matrix) and MrBayes 3.1.2 (Huelsenbeck and Ronquist, 2001) with the following parameters: ngen = 1×10^6, aamodel = mixed. These trees were then compared using the Shimodaira and Hasegawa (1999) and one-sided Kishino and Hasegawa (1989) tests, which calculate the likelihood of each tree, using maximum likelihood distances and the Jones-Taylor-Thornton amino acid substitution model. *P* values were obtained by a χ^2 test (Strimmer and Rambaut, 2002).

Comparison of Kelch Repeats within and between Proteins

Genetic distances among different kelch repeats within the same protein and among different proteins were estimated using protdist from the PHYLIP suite (Felsenstein, 1989). A permutation test was performed to estimate whether the similarity of kelch repeats within a protein is significantly lower than between proteins. As test statistic, the difference of the means and 1 million permutations was used. Test statistic d was defined as follows: d = mean (simKwP) – mean(simKbP), with simKwP as similarities of kelch repeats within a protein and simKbP as similarities of kelch repeats between different proteins (increasing similarity is denoted by decreasing simKxP values). A value of $d > 0$ means a lower similarity of repeats within proteins in contrast to repeats between proteins. Subsequently, the *P* value was calculated as the relative frequency of all random values greater than or equal to our measured value. Calculations were performed with R version 2.10.0 (Suzuki and Shimodaira, 2006).

Estimation of the Maximum Number of Gained and Lost FBKs

To determine the degrees of gene family expansion in the analyzed plant lineages, we divided the phylogeny into ancestral clades (those containing at least one representative of the lower land plants, monocots, and eudicots), recent clades (monocot specific, eudicot specific, or lower land plant specific), and species-specific clades. Nodes basal to the split among lineages denote the MRCA and are labeled as N1 to N5. In Figure 3, N0 was added as eukaryotic MRCA on basis of FBKs identified in Supplemental Table S2.

Divergence Levels and Sliding Window Analysis

For analysis of K_a/K_s ratios and sliding window plots, orthologous *A. thaliana* and *Arabidopsis lyrata* protein sequences were identified in Supplemental Figure S7. *A. thaliana*-*A. lyrata* gene pairs were considered orthologs when they clearly formed a single subclade and possible *A. lyrata* paralogs were more distantly related. Homologous protein sequences were aligned using ClustalW (Thompson et al., 2002). Codon alignments generated with PAL2NAL (Suyama et al., 2006) were used to compute divergence levels (K_a/K_s ratios) with DnaSP 5.0 (Librado and Rozas, 2009) using the sliding window option (window size, 150 bp; step size, 9 bp).

Correlation Analysis of Expression Data

To create the dendrogram for the cluster analysis of the expression data, the R package pvclust (Suzuki and Shimodaira, 2006) was used. The expression data of the *A. thaliana FBK*s were extracted from the AtGenExpress extended tissue series (Schmid et al., 2005). Only 81 of 103 *A. thaliana FBK*s were represented on the ATH1 microarray. In pvclust, a hierarchical clustering was performed using the Pearson correlation as a similarity measurement (dist = 1 – cor[x,y]) between the expression of the genes and the UPGMA method as cluster distance function. To calculate the stability of the dendrogram, a bootstrapping with 1,000 repeats was performed.

Measurement of Relative Transcript Levels by Quantitative Reverse Transcription-PCR in *A. thaliana*

Shoots were harvested from 7-d-old seedlings and roots from 10-d-old seedlings. Ecotype Columbia-0 seedlings were cultivated on sterile *A. thaliana* solution agar medium (Lincoln et al., 1990). After 2 d of stratification, the seedlings were cultivated under long-day conditions (16 h of light/8 h of dark) at 20°C. Additionally, 5-week-old Columbia-0 plants were cultivated in growth chambers under long-day conditions at 20°C, and cauline leaves, rosette leaves, open flowers, flower buds, stems, and siliques were harvested for RNA isolation. RNA isolation, cDNA synthesis, and quantitative reverse transcription-PCR were performed according to Delker et al. (2010). Gene-specific primer sequences can be found in Supplemental Table S6.

Subcellular Localization

To examine the subcellular localization of *A. thaliana* FBKs, 35S::GFP-FBK fusion constructs were created using the Gateway cloning system (Invitrogen) according to the manufacturer's protocols. pDONR221 was used as entry vector and pGWB6 (Nakagawa et al., 2007) as destination vector. Using *Agrobacterium tumefaciens* strain GV3101, the fusion constructs were transiently transformed into leaves of 6-week-old *Nicotiana benthamiana* plants grown in the greenhouse at 20°C and long-day conditions. GFP fluorescence was detected by confocal laser scanning microscopy (LSM510 META; Zeiss).

Yeast Two-Hybrid Assays

Initially, the *ASK* and *FBK* genes were cloned into pDONR221 vectors using the Gateway cloning system (Invitrogen) according to the manufacturer's protocols. The inserts were then recombined into "gatewayized" pGADT7, resulting in the expression of a GAL4 activation domain (AD) fusion protein. ASK constructs were cloned into pGBST7, resulting in the expression of a GAL4 DNA-binding domain (BD) fusion protein. Fusion constructs were transformed into *Saccharomyces cerevisiae* haploid strains AH109 (MATa; Invitrogen; James et al., 1996) and Y187 (MATα; Invitrogen; Harper et al., 1993). Following yeast mating, a dilution series of the diploid yeast cell suspension was grown at 30°C for 3 d on nonselective (−Leu, −Trp) and strong selective (−Leu, −Trp, −His, −Ade) media. To exclude autoactivation, all FBK and ASK constructs were cloned into pGADT7 and plated on selective (−Leu, −Trp) media. As a negative control, we performed interaction studies with human LaminC, which neither forms complexes nor interacts with most other proteins (Bartel et al., 1993; Ye and Worman, 1995).

Supplemental Data

The following materials are available in the online version of this article.

Supplemental Figure S1. Schematic view of a plant F-box kelch protein.

Supplemental Figure S2. Alignment of F-box associated domains and individual kelch repeats from *A. thaliana* proteins.

Supplemental Figure S3. Rooted NJ trees including FBKs and FBAs of *V. vinifera*, *P. trichocarpa*, *O. sativa*, *S. bicolor*, and *S. moellendorffii*.

Supplemental Figure S4. NJ tree generated using full-length FBK protein sequences of *A. thaliana*, *P. trichocarpa*, *V. vinifera*, *O. sativa*, *S. bicolor*, *S. moellendorffii*, and *P. patens*.

Supplemental Figure S5. Representative phylogenetic trees.

Supplemental Figure S6. Protein sequence alignment of 43 representative FBKs.

Supplemental Figure S7. NJ tree of *A. thaliana* and *A. lyrata* FBKs.

Supplemental Figure S8. Density plot of the permutation test.

Supplemental Figure S9. Relative transcript level of closely related FBKs.

Supplemental Table S1. Identifiers of F-box kelch proteins in *A. thaliana*, *P. trichocarpa*, *V. vinifera*, *O. sativa*, *S. bicolor*, *S. moellendorffii*, and *P. patens*.

Supplemental Table S2. Number of F-box kelch proteins in nonplant model species.

Supplemental Table S3. Identifiers of F-box proteins with F-box associated domains in *A. thaliana*, *P. trichocarpa*, *V. vinifera*, *O. sativa*, *S. bicolor*, *S. moellendorffii*, and *P. patens*.

Supplemental Table S4. Comparison of three tree topologies obtained with NJ, maximum likelihood, and Bayesian algorithms.

Supplemental Table S5. Absolute numbers of unstable, stable, ancient, and superstable FBKs in plant genomes.

Supplemental Table S6. Sequences of quantitative reverse transcription-PCR primers.

Supplemental Data Set S1. Tissue-specific expression data of *A. thaliana* FBKs extracted from AtGenExpress_Plus extended tissue series.

ACKNOWLEDGMENTS

We thank the members of the Quint laboratory, Doug Grubb, and two anonymous reviewers for helpful comments on the manuscript and Thomas Lahaye for yeast strains and vectors. Furthermore, we are grateful to Mariana Mondragon-Palomino for her phylogenetic expertise, to Anja Raschke and Nina Dombrowski for technical support, and to Wolfgang Knogge and Steffen Neumann.

Received September 30, 2010; accepted November 24, 2010; published November 30, 2010.

LITERATURE CITED

Adams J, Kelso R, Cooley L (2000) The kelch repeat superfamily of proteins: propellers of cell function. Trends Cell Biol **10:** 17–24

Altschul SF, Madden TL, Schäffer AA, Zhang J, Zhang Z, Miller W, Lipman DJ (1997) Gapped BLAST and PSI-BLAST: a new generation of protein database search programs. Nucleic Acids Res **25:** 3389–3402

An F, Zhao Q, Ji Y, Li W, Jiang Z, Yu X, Zhang C, Han Y, He W, Liu Y, et al (2010) Ethylene-induced stabilization of ETHYLENE INSENSITIVE3 and EIN3-LIKE1 is mediated by proteasomal degradation of EIN3 binding F-box 1 and 2 that requires EIN2 in *Arabidopsis*. Plant Cell **22:** 2384–2401

Andrade MA, González-Guzmán M, Serrano R, Rodríguez PL (2001) A combination of the F-box motif and kelch repeats defines a large Arabidopsis family of F-box proteins. Plant Mol Biol **46:** 603–614

Bartel P, Chien CT, Sternglanz R, Fields S (1993) Elimination of false positives that arise in using the two-hybrid system. Biotechniques **14:** 920–924

Baudry A, Ito S, Song YH, Strait AA, Kiba T, Lu S, Henriques R, Pruneda-Paz JL, Chua NH, Tobin EM, et al (2010) F-box proteins FKF1 and LKP2 act in concert with ZEITLUPE to control *Arabidopsis* clock progression. Plant Cell **22:** 606–622

Binder BM, Walker JM, Gagné JM, Emborg TJ, Hemmann G, Bleecker AB, Vierstra RD (2007) The *Arabidopsis* EIN3 binding F-box proteins EBF1 and EBF2 have distinct but overlapping roles in ethylene signaling. Plant Cell **19:** 509–523

Blanc G, Hokamp K, Wolfe KH (2003) A recent polyploidy superimposed on older large-scale duplications in the Arabidopsis genome. Genome Res **13:** 137–144

Book AJ, Smalle J, Lee KH, Yang P, Walker JM, Casper S, Holmes JH, Russo LA, Buzzinotti ZW, Jenik PD, Vierstra RD (2009) The RPN5 subunit of the 26s proteasome is essential for gametogenesis, sporophyte development, and complex assembly in *Arabidopsis*. Plant Cell **21:** 460–478

Bork P, Doolittle RF (1994) Drosophila kelch motif is derived from a common enzyme fold. J Mol Biol **236:** 1277–1282

Bowers JE, Chapman BA, Rong JK, Paterson AH (2003) Unravelling angiosperm genome evolution by phylogenetic analysis of chromosomal duplication events. Nature **422:** 433–438

Cardozo T, Pagano M (2004) The SCF ubiquitin ligase: insights into a molecular machine. Nat Rev Mol Cell Biol **5:** 739–751

Chae E, Tan QK, Hill TA, Irish VF (2008) An Arabidopsis F-box protein acts as a transcriptional co-factor to regulate floral development. Development **135:** 1235–1245

Clark RM, Schweikert G, Toomajian C, Ossowski S, Zeller G, Shinn P, Warthmann N, Hu TT, Fu G, Hinds DA, et al (2007) Common sequence polymorphisms shaping genetic diversity in *Arabidopsis thaliana*. Science **317:** 338–342

Delker C, Pöschl Y, Raschke A, Ullrich K, Ettingshausen S, Hauptmann V, Grosse I, Quint M (2010) Natural variation of transcriptional auxin response networks in *Arabidopsis thaliana*. Plant Cell **22:** 2184–2200

Demarsy E, Fankhauser C (2009) Higher plants use LOV to perceive blue light. Curr Opin Plant Biol **12:** 69–74

Demuth JP, Hahn MW (2009) The life and death of gene families. Bioessays **31:** 29–39

Dharmasiri N, Dharmasiri S, Weijers D, Lechner E, Yamada M, Hobbie L, Ehrismann JS, Jürgens G, Estelle M (2005) Plant development is regulated by a family of auxin receptor F box proteins. Dev Cell **9:** 109–119

Dill A, Thomas SG, Hu J, Steber CM, Sun TP (2004) The *Arabidopsis* F-box protein SLEEPY1 targets gibberellin signaling repressors for gibberellin-induced degradation. Plant Cell **16:** 1392–1405

Dong L, Wang L, Zhang Y, Zhang Y, Deng X, Xue Y (2006) An auxin-inducible F-box protein CEGENDUO negatively regulates auxin-mediated lateral root formation in Arabidopsis. Plant Mol Biol **60:** 599–615

Du ZY, Xiao S, Chen QF, Chye ML (2010) Depletion of the membrane-associated acyl-coenzyme A-binding protein ACBP1 enhances the ability of cold acclimation in Arabidopsis. Plant Physiol **152:** 1585–1597

Eddy SR (1998) Profile hidden Markov models. Bioinformatics **14:** 755–763

Felsenstein J (1989) PHYLIP: Phylogeny Inference Package (version 3.2). Cladistics **5:** 164–166

Fukamatsu Y, Mitsui S, Yasuhara M, Tokioka Y, Ihara N, Fujita S, Kiyosue T (2005) Identification of LOV KELCH PROTEIN2 (LKP2)-interacting factors that can recruit LKP2 to nuclear bodies. Plant Cell Physiol **46:** 1340–1349

Fülöp V, Jones DT (1999) Beta propellers: structural rigidity and functional diversity. Curr Opin Struct Biol **9:** 715–721

Gagné JM, Downes BP, Shiu SH, Durski AM, Vierstra RD (2002) The F-box subunit of the SCF E3 complex is encoded by a diverse superfamily of genes in Arabidopsis. Proc Natl Acad Sci USA **99:** 11519–11524

González-Carranza ZH, Rompa U, Peters JL, Bhatt AM, Wagstaff C, Stead AD, Roberts JA (2007) Hawaiian skirt: an F-box gene that regulates organ fusion and growth in Arabidopsis. Plant Physiol **144:** 1370–1382

Gou M, Su N, Zheng J, Huai J, Wu G, Zhao J, He J, Tang D, Yang S, Wang G (2009) An F-box gene, CPR30, functions as a negative regulator of the defense response in Arabidopsis. Plant J **60:** 757–770

Gough J, Karplus K, Hughey R, Chothia C (2001) Assignment of homology to genome sequences using a library of hidden Markov models that represent all proteins of known structure. J Mol Biol **313:** 903–919

Guo H, Ecker JR (2003) Plant responses to ethylene gas are mediated by SCF(EBF1/EBF2)-dependent proteolysis of EIN3 transcription factor. Cell **115:** 667–677

Han L, Mason M, Risseeuw EP, Crosby WL, Somers DE (2004) Formation of an SCF(ZTL) complex is required for proper regulation of circadian timing. Plant J **40:** 291–301

Hanada K, Zou C, Lehti-Shiu MD, Shinozaki K, Shiu SH (2008) Importance of lineage-specific expansion of plant tandem duplicates in the adaptive response to environmental stimuli. Plant Physiol **148:** 993–1003

Harmon FG, Kay SA (2003) The F box protein AFR is a positive regulator of phytochrome A-mediated light signaling. Curr Biol **13:** 2091–2096

Harper JW, Adami GR, Wei N, Keyomarsi K, Elledge SJ (1993) The p21 Cdk-interacting protein Cip1 is a potent inhibitor of G1 cyclin-dependent kinases. Cell **75:** 805–816

Hermand D (2006) F-box proteins: more than baits for the SCF? Cell Div **1:** 30

Huelsenbeck JP, Ronquist F (2001) MRBAYES: Bayesian inference of phylogenetic trees. Bioinformatics **17:** 754–755

Jain M, Nijhawan A, Arora R, Agarwal P, Ray S, Sharma P, Kapoor S, Tyagi AK, Khurana JP (2007) F-box proteins in rice: genome-wide analysis, classification, temporal and spatial gene expression during panicle and seed development, and regulation by light and abiotic stress. Plant Physiol **143:** 1467–1483

James P, Halladay J, Craig EA (1996) Genomic libraries and a host strain designed for highly efficient two-hybrid selection in yeast. Genetics **144:** 1425–1436

Jaso-Friedmann L, Peterson DS, Gonzalez DS, Evans DL (2002) The antigen receptor (NCCRP-1) on catfish and zebrafish nonspecific cytotoxic cells belongs to a new gene family characterized by an F-box-associated domain. J Mol Evol **54:** 386–395

Jawad Z, Paoli M (2002) Novel sequences propel familiar folds. Structure **10:** 447–454

Jin J, Cardozo T, Lovering RC, Elledge SJ, Pagano M, Harper JW (2004) Systematic analysis and nomenclature of mammalian F-box proteins. Genes Dev **18:** 2573–2580

Kenrick P, Crane PR (1997) The origin and early evolution of plants on land. Nature **389:** 33–39

Kim HS, Delaney TP (2002) *Arabidopsis* SON1 is an F-box protein that regulates a novel induced defense response independent of both salicylic acid and systemic acquired resistance. Plant Cell **14:** 1469–1482

Kim OK, Jung JH, Park CM (2010) An Arabidopsis F-box protein regulates tapetum degeneration and pollen maturation during anther development. Planta **232:** 353–366

Kim WY, Fujiwara S, Suh SS, Kim J, Kim Y, Han L, David K, Putterill J, Nam HG, Somers DE (2007) ZEITLUPE is a circadian photoreceptor stabilized by GIGANTEA in blue light. Nature **449:** 356–360

Kipreos ET, Pagano M (2000) The F-box protein family. Genome Biol **1:** REVIEWS3002

Kishino H, Hasegawa M (1989) Evaluation of the maximum likelihood estimate of the evolutionary tree topologies from DNA sequence data, and the branching order in Hominoidea. J Mol Evol **29:** 170–179

Lechner E, Achard P, Vansiri A, Potuschak T, Genschik P (2006) F-box proteins everywhere. Curr Opin Plant Biol **9:** 631–638

Leung KC, Li HY, Mishra G, Chye ML (2004) ACBP4 and ACBP5, novel Arabidopsis acyl-CoA-binding proteins with kelch motifs that bind oleoyl-CoA. Plant Mol Biol **55:** 297–309

Li X, Zhang D, Hannink M, Beamer LJ (2004) Crystal structure of the kelch domain of human Keap1. J Biol Chem **279:** 54750–54758

Librado P, Rozas J (2009) DnaSP v5: a software for comprehensive analysis of DNA polymorphism data. Bioinformatics **25:** 1451–1452

Lincoln C, Britton JH, Estelle M (1990) Growth and development of the *axr1* mutants of *Arabidopsis*. Plant Cell **2:** 1071–1080

Mazzucotelli E, Belloni S, Marone D, De Leonardis A, Guerra D, Di Fonzo N, Cattivelli L, Mastrangelo A (2006) The e3 ubiquitin ligase gene family in plants: regulation by degradation. Curr Genomics **7:** 509–522

Mora-García S, Vert G, Yin Y, Caño-Delgado A, Cheong H, Chory J (2004) Nuclear protein phosphatases with kelch-repeat domains modulate the response to brassinosteroids in Arabidopsis. Genes Dev **18:** 448–460

Nakagawa T, Kurose T, Hino T, Tanaka K, Kawamukai M, Niwa Y, Toyooka K, Matsuoka K, Jinbo T, Kimura T (2007) Development of series of Gateway binary vectors, pGWBs, for realizing efficient construction of fusion genes for plant transformation. J Biosci Bioeng **104:** 34–41

Ou CY, Pi H, Chien CT (2003) Control of protein degradation by E3 ubiquitin ligases in *Drosophila* eye development. Trends Genet **19:** 382–389

Parry G, Calderon-Villalobos LI, Prigge M, Peret B, Dharmasiri S, Itoh H, Lechner E, Gray WM, Bennett M, Estelle M (2009) Complex regulation of the TIR1/AFB family of auxin receptors. Proc Natl Acad Sci USA **106:** 22540–22545

Prag S, Adams JC (2003) Molecular phylogeny of the kelch-repeat superfamily reveals an expansion of BTB/kelch proteins in animals. BMC Bioinformatics **4:** 42

Qiao H, Chang KN, Yazaki J, Ecker JR (2009) Interplay between ethylene, ETP1/ETP2 F-box proteins, and degradation of EIN2 triggers ethylene responses in Arabidopsis. Genes Dev **23:** 512–521

Risseeuw EP, Daskalchuk TE, Banks TW, Liu E, Cotelesage J, Hellmann H, Estelle M, Somers DE, Crosby WL (2003) Protein interaction analysis of SCF ubiquitin E3 ligase subunits from Arabidopsis. Plant J **34:** 753–767

Rubin GM, Yandell MD, Wortman JR, Gabor Miklos GL, Nelson CR, Hariharan IK, Fortini ME, Li PW, Apweiler R, Fleischmann W, et al (2000) Comparative genomics of the eukaryotes. Science **287:** 2204–2215

Ruegger M, Dewey E, Gray WM, Hobbie L, Turner J, Estelle M (1998) The TIR1 protein of Arabidopsis functions in auxin response and is related to human SKP2 and yeast grr1p. Genes Dev **12:** 198–207

Sawa M, Nusinow DA, Kay SA, Imaizumi T (2007) FKF1 and GIGANTEA complex formation is required for day-length measurement in Arabidopsis. Science **318:** 261–265

Schmid M, Davison TS, Henz SR, Pape UJ, Demar M, Vingron M, Schölkopf B, Weigel D, Lohmann JU (2005) A gene expression map of *Arabidopsis thaliana* development. Nat Genet **37:** 501–506

Schwager KM, Calderon-Villalobos LIA, Dohmann EMN, Willige BC, Knierer S, Nill C, Schwechheimer C (2007) Characterization of the VIER F-BOX PROTEINE genes from *Arabidopsis* reveals their importance for plant growth and development. Plant Cell **19:** 1163–1178

Seki M, Narusaka M, Kamiya A, Ishida J, Satou M, Sakurai T, Nakajima M, Enju A, Akiyama K, Oono Y, et al (2002) Functional annotation of a full-length Arabidopsis cDNA collection. Science **296:** 141–145

Shimodaira H, Hasegawa M (1999) Multiple comparisons of log-likelihoods with applications to phylogenetic inference. Mol Biol Evol **16:** 1114–1116

Skaar JR, D'Angiolella V, Pagan JK, Pagano M (2009a) SnapShot: F box proteins II. Cell **137:** 1358

Skaar JR, Pagan JK, Pagano M (2009b) SnapShot: F box proteins I. Cell **137:** 1160

Sonnhammer EL, Eddy SR, Durbin R (1997) Pfam: a comprehensive database of protein domain families based on seed alignments. Proteins **28:** 405–420

Sterck L, Rombauts S, Jansson S, Sterky F, Rouzé P, Van de Peer Y (2005) EST data suggest that poplar is an ancient polyploid. New Phytol **167:** 165–170

Stone SL, Callis J (2007) Ubiquitin ligases mediate growth and development by promoting protein death. Curr Opin Plant Biol **10:** 624–632

Strimmer K, Rambaut A (2002) Inferring confidence sets of possibly misspecified gene trees. Proc Biol Sci **269:** 137–142

Sun L, Shi L, Li W, Yu W, Liang J, Zhang H, Yang X, Wang Y, Li R, Yao X, et al (2009) JFK, a kelch domain-containing F-box protein, links the SCF complex to p53 regulation. Proc Natl Acad Sci USA **106:** 10195–10200

Suyama M, Torrents D, Bork P (2006) PAL2NAL: robust conversion of protein sequence alignments into the corresponding codon alignments. Nucleic Acids Res **34:** W609–W612

Suzui N, Nakamura S, Fujiwara T, Hayashi H, Yoneyama T (2006) A putative acyl-CoA-binding protein is a major phloem sap protein in rice (*Oryza sativa* L.). J Exp Bot **57:** 2571–2576

Suzuki R, Shimodaira H (2006) Pvclust: an R package for assessing the uncertainty in hierarchical clustering. Bioinformatics **22:** 1540–1542

Takahashi N, Kuroda H, Kuromori T, Hirayama T, Seki M, Shinozaki K, Shimada H, Matsui M (2004) Expression and interaction analysis of Arabidopsis Skp1-related genes. Plant Cell Physiol **45:** 83–91

Thomas JH (2006) Adaptive evolution in two large families of ubiquitin-ligase adapters in nematodes and plants. Genome Res **16:** 1017–1030

Thompson JD, Gibson TJ, Higgins DG (2002) Multiple sequence alignment using ClustalW and ClustalX. Curr Protoc Bioinformatics **August:** chapter 2, unit 2.3

Toufighi K, Brady SM, Austin R, Ly E, Provart NJ (2005) The Botany Array Resource: e-northerns, expression angling, and promoter analyses. Plant J **43:** 153–163

Tuskan GA, Difazio S, Jansson S, Bohlmann J, Grigoriev I, Hellsten U, Putnam N, Ralph S, Rombauts S, Salamov A, et al (2006) The genome of black cottonwood, *Populus trichocarpa* (Torr. & Gray). Science **313:** 1596–1604

Vierstra RD (2009) The ubiquitin-26S proteasome system at the nexus of plant biology. Nat Rev Mol Cell Biol **10:** 385–397

Wang L, Dong L, Zhang Y, Zhang Y, Wu W, Deng X, Xue Y (2004) Genome-wide analysis of S-locus F-box-like genes in *Arabidopsis thaliana*. Plant Mol Biol **56:** 929–945

Weigel D, Mott R (2009) The 1001 genomes project for Arabidopsis thaliana. Genome Biol **10:** 107

Woo HR, Chung KM, Park JH, Oh SA, Ahn T, Hong SH, Jang SK, Nam HG (2001) ORE9, an F-box protein that regulates leaf senescence in *Arabidopsis*. Plant Cell **13:** 1779–1790

Xu G, Ma H, Nei M, Kong H (2009) Evolution of F-box genes in plants: different modes of sequence divergence and their relationships with functional diversification. Proc Natl Acad Sci USA **106:** 835–840

Xu L, Liu F, Lechner E, Genschik P, Crosby WL, Ma H, Peng W, Huang D, Xie D (2002) The SCF(COI1) ubiquitin-ligase complexes are required for jasmonate response in *Arabidopsis*. Plant Cell **14:** 1919–1935

Xue F, Cooley L (1993) Kelch encodes a component of intercellular bridges in *Drosophila* egg chambers. Cell **72:** 681–693

Yang X, Kalluri UC, Jawdy S, Gunter LE, Yin T, Tschaplinski TJ, Weston DJ, Ranjan P, Tuskan GA (2008) The F-box gene family is expanded in herbaceous annual plants relative to woody perennial plants. Plant Physiol **148:** 1189–1200

Ye Q, Worman HJ (1995) Protein-protein interactions between human nuclear lamins expressed in yeast. Exp Cell Res **219:** 292–298

Supplemental Data

Supplemental Figure S1. Schematic view of a plant F-box kelch protein.

Supplemental Figure S2. Alignment of F-box associated domains and individual kelch repeats from *A. thaliana* proteins.

Supplemental Figure S3. Rooted NJ trees including FBKs and FBAs of *V. vinifera*, *P. trichocarpa*, *O. sativa, S. bicolor* and *S. moellendorffii*.

Supplemental Figure S4. NJ tree generated using full-length FBK protein sequences of *A. thaliana*, *P. trichocarpa*, *V. vinifera*, *O. sativa*, *S. bicolor*, *S. moellendorffii* and *P. patens*.

Supplemental Figure S5. Representative phylogenetic trees.

Supplemental Figure S6. Protein sequence alignment of 43 representative FBKs.

Supplemental Figure S7. NJ tree of *A. thaliana* and *A. lyrata* FBKs.

Supplemental Figure S8. Density plot of the permutation test.

Supplemental Figure S9. Relative transcript level of closely related FBKs.

Supplemental Table S1. Identifiers of F-box kelch proteins in *A. thaliana*, *P. trichocarpa*, *V. vinifera*, *O. sativa*, *S. bicolor*, *S. moellendorffii* and *P. patens*.

Supplemental Table S2. Number of F-box kelch proteins in non-plant model species.

Supplemental Table S3. Identifiers of F-box proteins with F-box associated domains in *A. thaliana*, *P. trichocarpa, V. vinifera*, *O. sativa*, *S. bicolor*, *S. moellendorffii* and *P. patens.*

Supplemental Table S4. Comparison of three tree topologies obtained with NJ, ML and Bayesian Algorithms.

Supplemental Table S5. Absolute numbers of unstable, stable, ancient and superstable FBKs in plant genomes.

Supplemental Table S6. Sequences of q-RT PCR primers.

Supplemental Dataset S1. Tissue-specific expression data of *A. thaliana* FBKs extracted from ATGenExpress_Plus – extended tissue series.

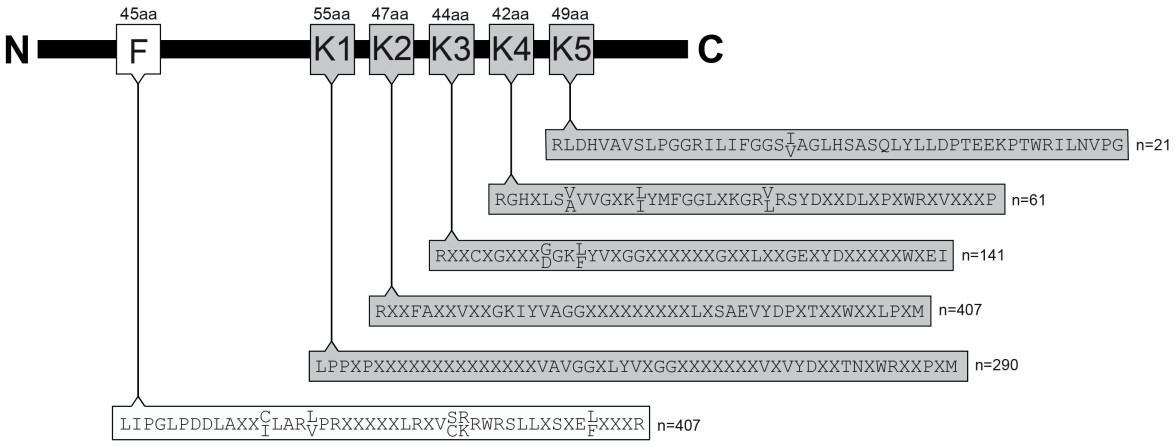

Supplemental Figure S1. Schematic view of a plant FBK protein. Consensus sequences of the F-box domain and kelch repeats are depicted below. In general, amino acids that share at least 30% homology between all sequences of an alignment are given in the one letter amino acid code, whereas amino acids with less than 30% homology are depicted as an "X". Exceptionally, in the case of the kelch 5 repeat amino acids with less than 50% homology are depicted as an "X". Gaps occuring in the alignment were deleted if more than 50% of the aligned sequences contained a gap at the same position. The positions of each domain within the alignment were determined using Pfam (Sonnhammer et al., 1997). n = number of sequences that underly the respective consensus sequence.

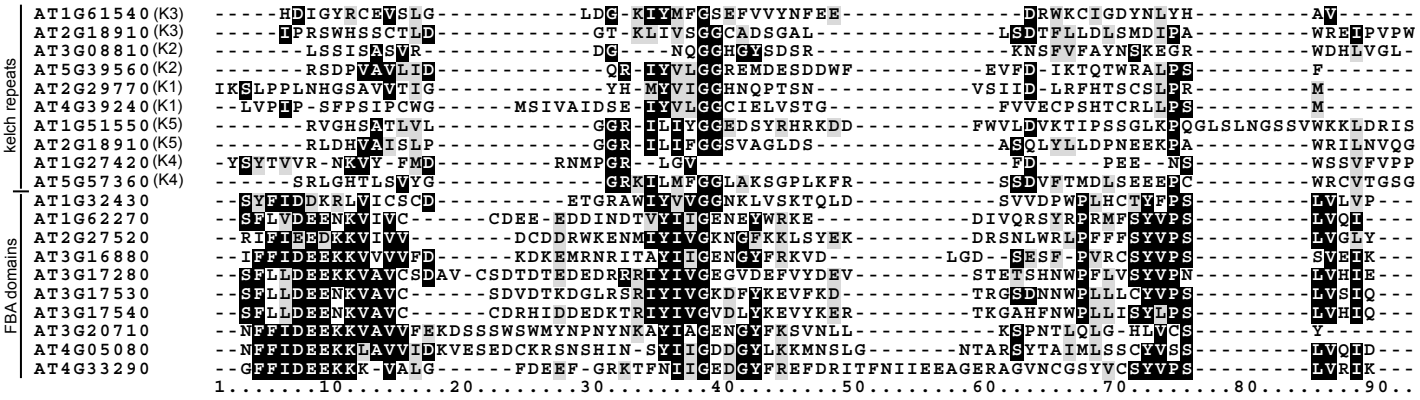

Supplemental Figure S2. Alignment of F-box associated domains and individual kelch repeats (K1-K5) from randomly chosen *A. thaliana* proteins obtained with ClustalX.

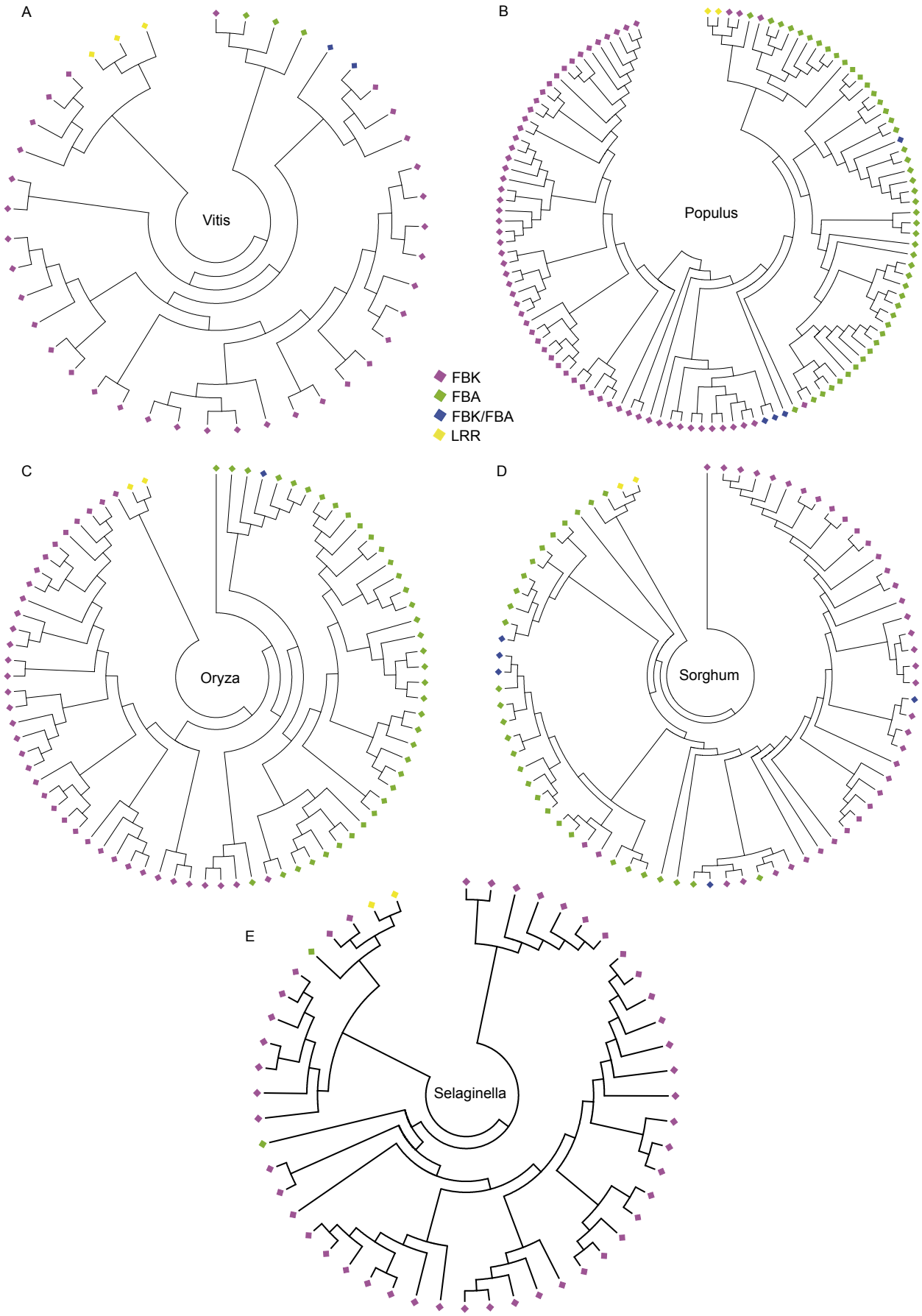

Supplemental Figure S3. FBKs and FBAs are closely related to each other. Rooted NJ trees including FBKs and FBAs of **A**: *V. vinifera*, **B**: *P. trichocarpa*, **C**: *O. sativa,* **D**: *S. bicolor* and **E**: *S. moellendorffii*. Alignment of full-length protein sequences and construction of the NJ trees was performed in MEGA, using a bootstrap value of 1000. Trees were rooted with leucine-rich repeat containing F-box proteins (LRRs) of the respective species identified by BlastP search with AtTIR1. FBK/FBA proteins are characterized by overlapping positions of the F-box associated domain and individual kelch repeats.

Supplemental Figure S4. NJ tree generated using full-length FBK protein sequences of *A. thaliana*, *P. trichocarpa*, *V. vinifera*, *O. sativa*, *S. bicolor*, *S. moellendorffii* and *P. patens*. Numbers at branches indicate bootstrap values >50. Color code indicates species background of the FBKs. The NJ tree was devided in 40 ortholog clades according to the bootstrap support and phylogenetic distances, respectively. Ortholog clades were categorized in (i) unstable: lineage-specific clades, (ii) stable: clades including orthologs in at least two species, (iii) ancient: clades including orthologs in at least one lower land plant, one monocot and one eudicot species, (iv) superstable: clades with orthologs in all analyzed land plant species.

A Maximum Likelihood

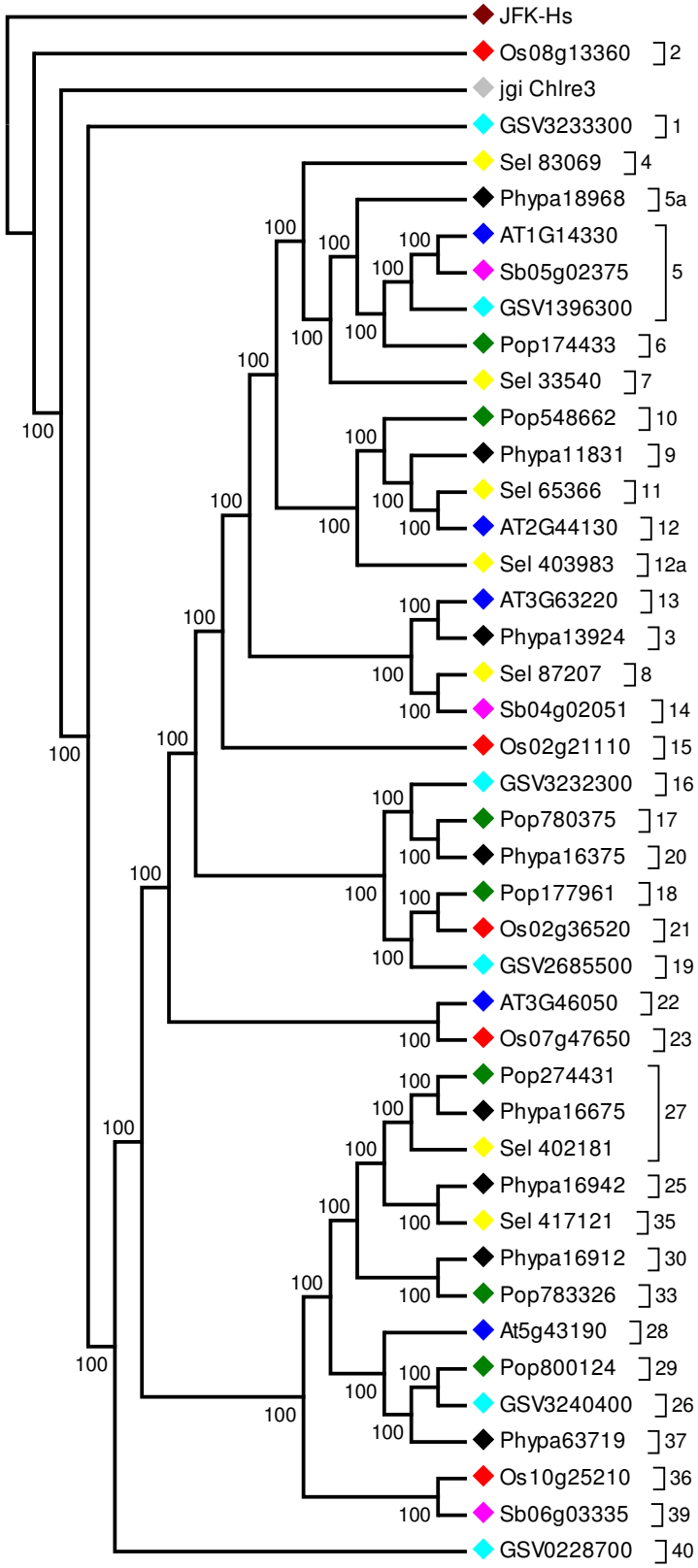

B Bayesian

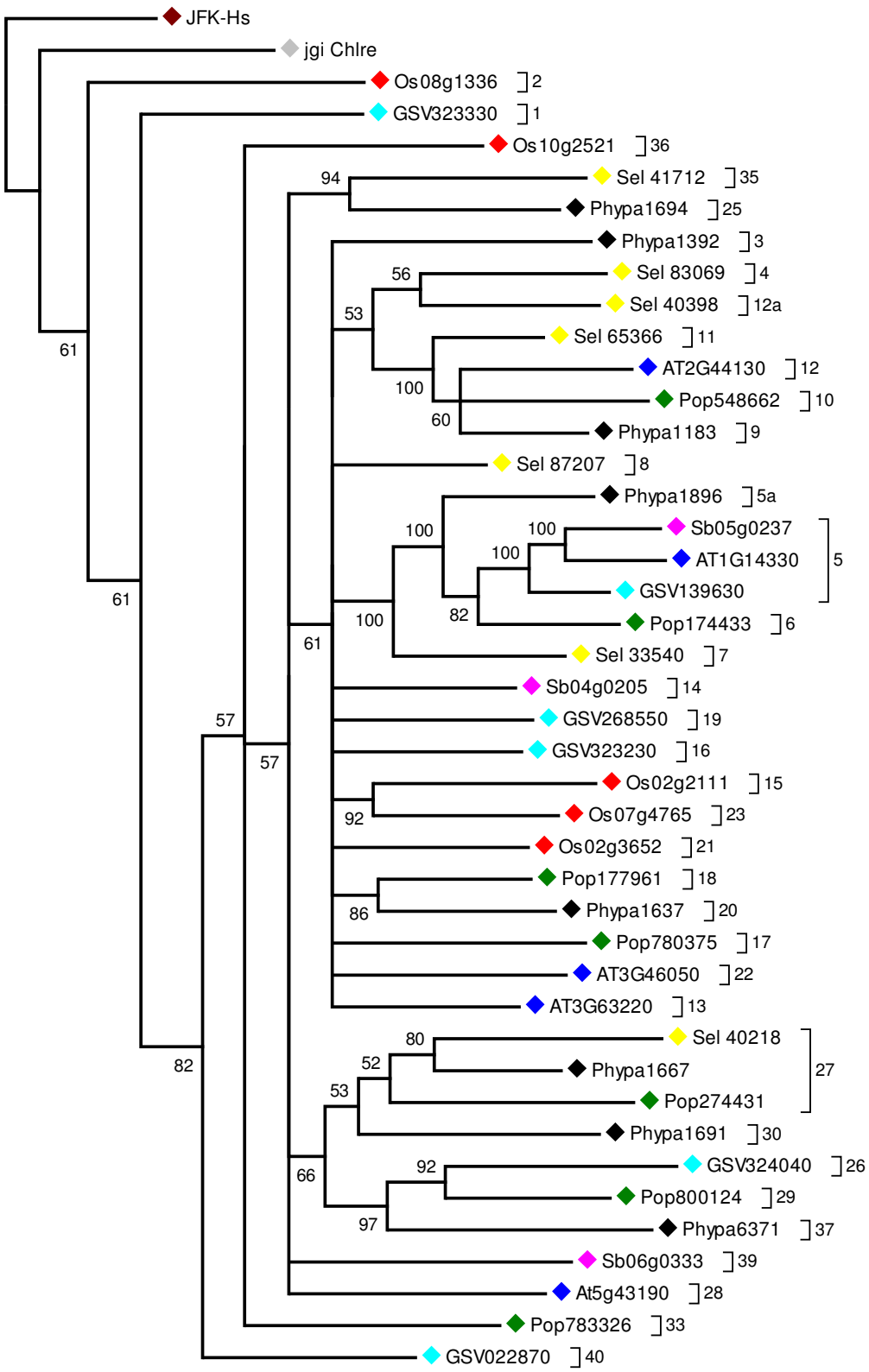
JFK-Hs
jgi Chlre
Os08g1336]2
GSV323330]1
Os10g2521]36
Sel 41712]35
Phypa1694]25
Phypa1392]3
Sel 83069]4
Sel 40398]12a
Sel 65366]11
AT2G44130]12
Pop548662]10
Phypa1183]9
Sel 87207]8
Phypa1896]5a
Sb05g0237
AT1G14330
GSV139630
5
Pop174433]6
Sel 33540]7
Sb04g0205]14
GSV268550]19
GSV323230]16
Os02g2111]15
Os07g4765]23
Os02g3652]21
Pop177961]18
Phypa1637]20
Pop780375]17
AT3G46050]22
AT3G63220]13
Sel 40218
Phypa1667
Pop274431
27
Phypa1691]30
GSV324040]26
Pop800124]29
Phypa6371]37
Sb06g0333]39
At5g43190]28
Pop783326]33
GSV022870]40
94
61
56
53
100
60
61
100
100
100
82
100
61
57
57
92
86
80
52
53
66
92
97
82

C Neighbor-joining

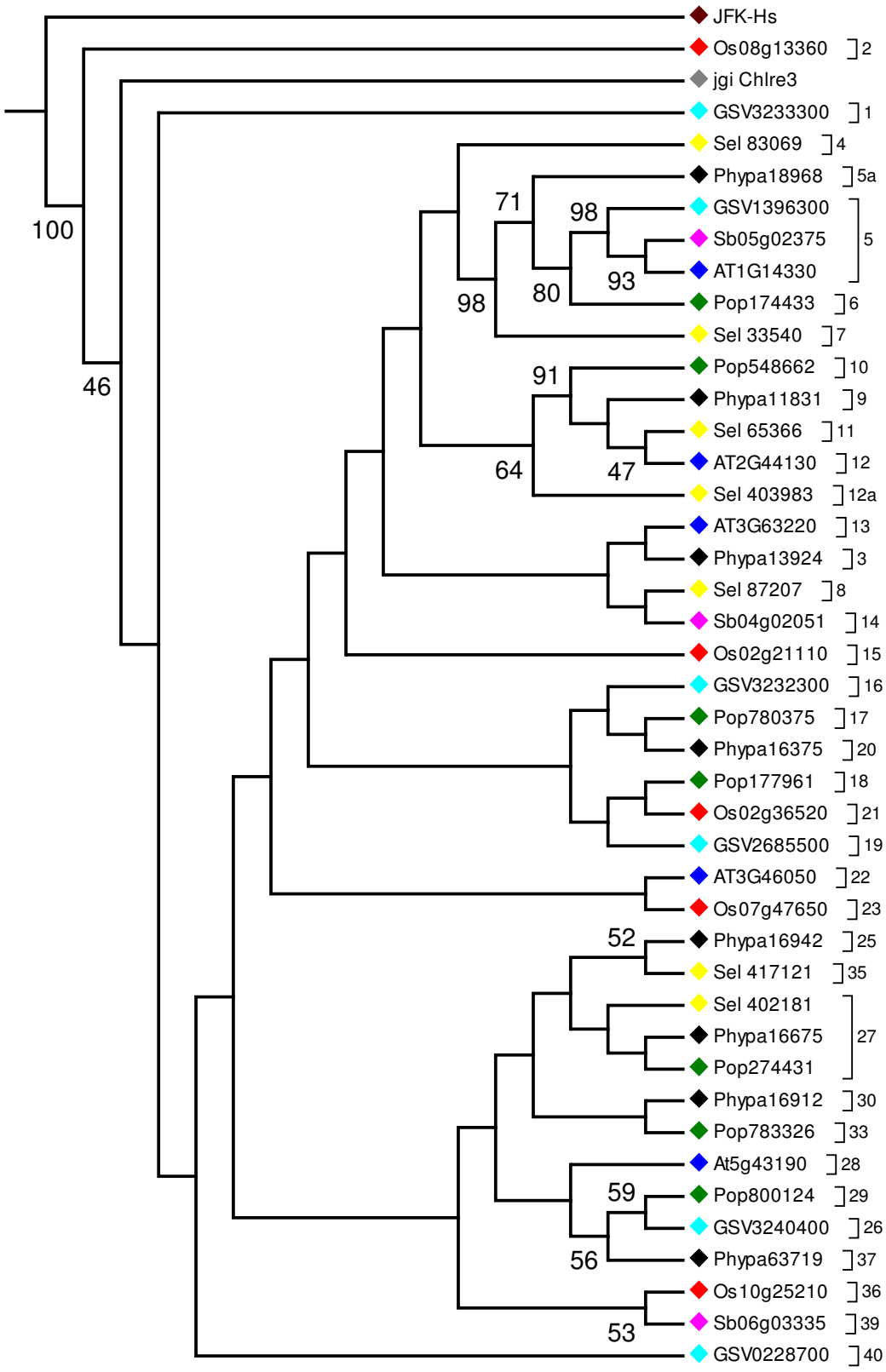

Supplemental Figure S5. Representative phylogenetic trees. **A**: Maximum likelihood (ML), **B**: Bayesian and **C**: Neighbor-Joining (NJ) trees from 43 representative FBK protein sequences. At least one sequence from each of the clades of the NJ tree from Supplementary Figure 4 was randomly sampled. The number of the clade from which the sequence was sampled is displayed after the bracket. Single sequences not belonging to a group of orthologs are labeled as clade #a. The Bayesian and NJ trees display numbers at the nodes that have bootstrap values >45%; the ML tree displays nodes with bootstrap values of 100%. Sequence names are abbreviated as in Supplemental Fig. S6.

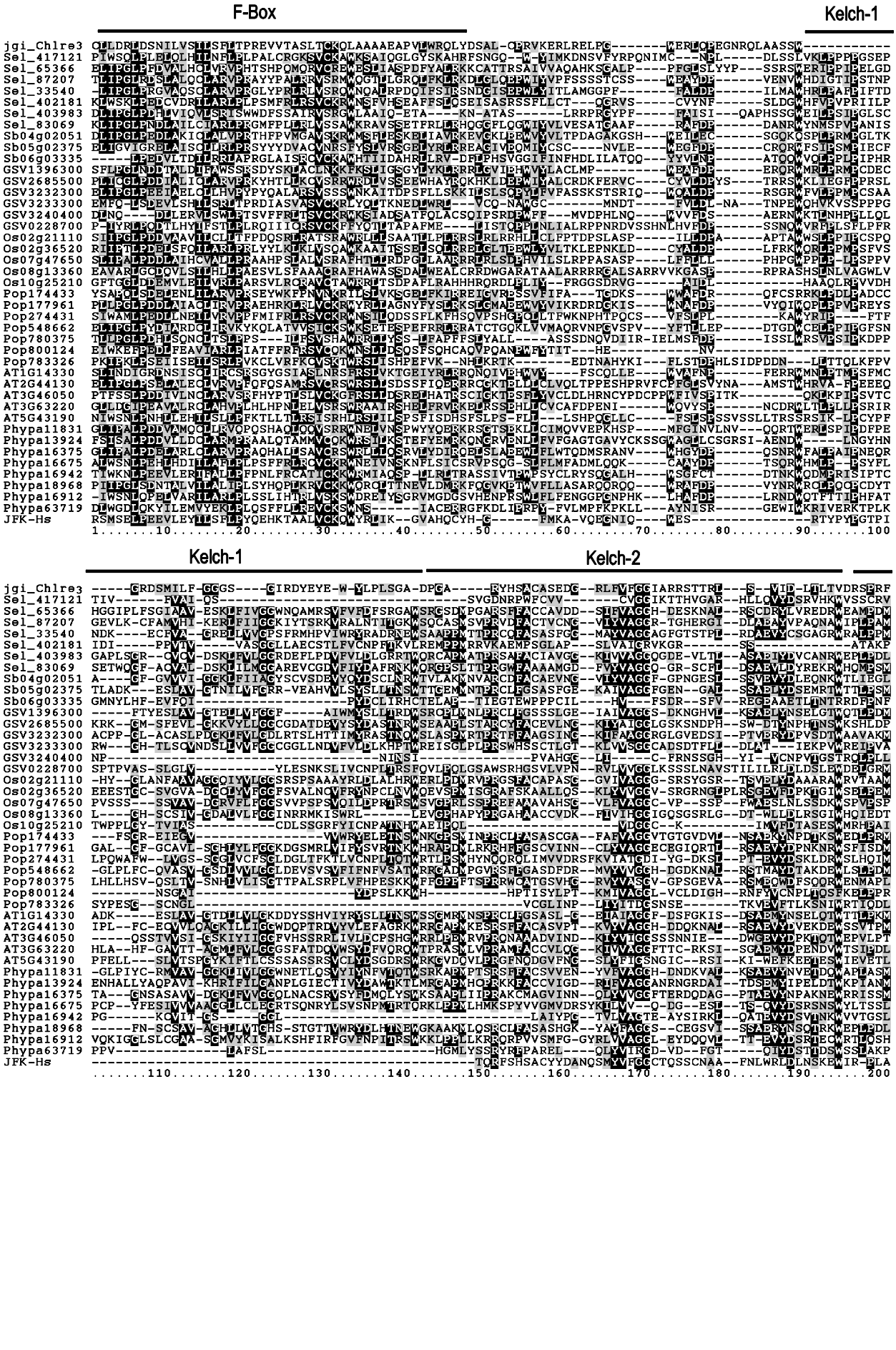
F-Box
Kelch-1
Kelch-1
Kelch-2
jgi_Chlre3
Sel_417121
Sel_65366
Sel_87207
Sel_33540
Sel_402181
Sel_403983
Sel_83069
Sb04g02051
Sb05g02375
Sb06g03335
GSV1396300
GSV2685500
GSV3232300
GSV3233300
GSV3240400
GSV0228700
Os02g21110
Os02g36520
Os07g47650
Os08g13360
Os10g25210
Pop174433
Pop177961
Pop274431
Pop548662
Pop780375
Pop800124
Pop783326
AT1G14330
AT2G44130
AT3G46050
AT3G63220
AT5G43190
Phypa11831
Phypa13924
Phypa16375
Phypa16675
Phypa16942
Phypa18968
Phypa16912
Phypa63719
JFK-Hs

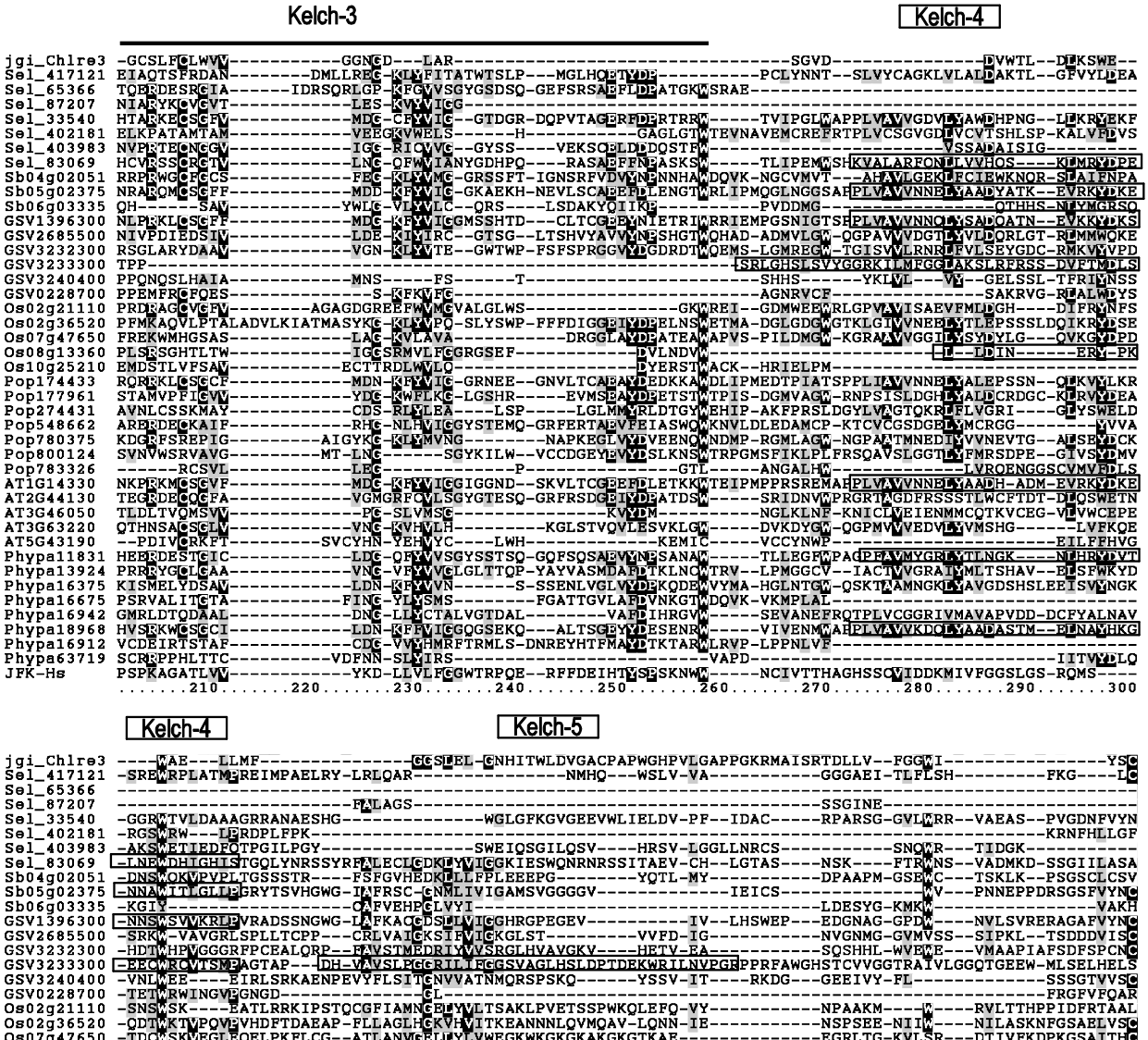
Kelch-3
Kelch-4
Kelch-4
Kelch-5

Supplemental Figure S6. Protein sequence alignment created with hmmalign of 43 representatives of the FBKs, where at least one sequence was sampled from each of the clades of the gene tree in Supplemental Fig. S4. Positions of F-box domain and kelch repeats are indicated with black bars on top of the alignment, except for kelch repeat 4 and 5, which are enclosed in a box inside the alignment. Sequence names are abbreviated for visualization purposes. Abbreviations are: Chlre= *Chlamydomonas reinhardtii* jgi#; Phypa= *Physcomitrella patens* #=jgi number; Selmo= *Selaginella moellendorffii* #=jgi number; Os# = *Oryza sativa* LOC_OS#, where # stands for locus number given at MSU (TIGR); Sb#= *Sorghum bicolor* (jgi); Pop_#= *Populus trichocarpa* #=jgi number; GSV #=Genoscope number first 7 digits; ATI code (TAIR) is used for *Arabidopsis thaliana*; JFK-Hs = *Homo sapiens* FBX42 (AAH43410.1).

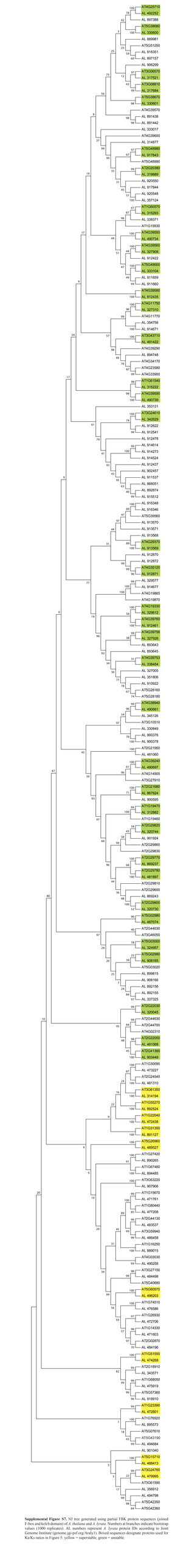

Supplemental Figure S7. NJ tree generated using partial FBK protein sequences (joined F-box and kelch domain) of *A. thaliana* and *A. lyrata*. Numbers at branches indicate bootstrap values (1000 replicates). AL numbers represent *A. lyrata* protein IDs according to Joint Genome Institute (genome.jgi-psf.org/Araly1). Boxed sequences designate proteins used for Ka/Ks ratios in Figure 5: yellow = superstable, green = unstable.

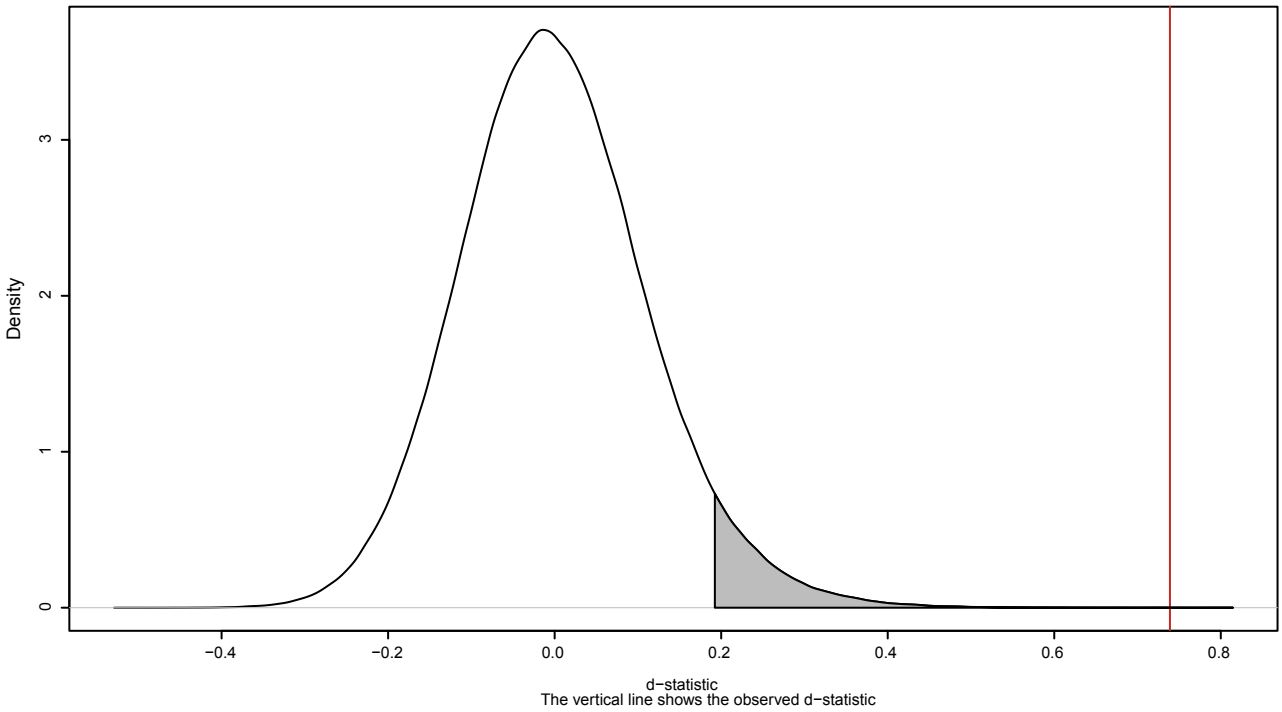

Supplemental Figure S8. Density plot of the test statistic d generated from the permutation test (one million repeats). D-statistic is defined as difference of the average means between the similarity of all kelch repeats within a protein and the similarity of kelch repeats between different proteins. Genetic distances among different kelch repeats were estimated using protdist from the PHYLIP suite (Felsenstein, 1989). The red line shows the d-statistic value for the observed arrangement of kelch repeats. The gray shaded area corresponds to the critical region (α=0.05), with a critical value of d as 0.1923.

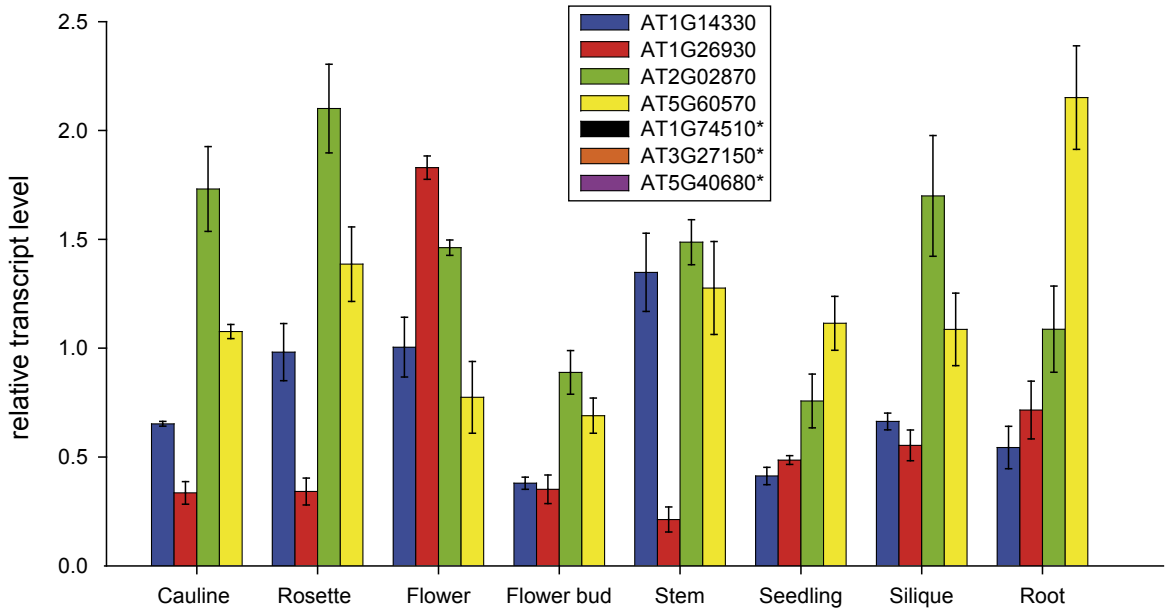

Supplemental Figure S9. Relative transcript level of a subset of closely related FBKs. Plant organs were harvested from 6-week-old *A. thaliana* Col-0 plants cultivated under long day conditions at 20°C. Seedlings were cultivated for 7 days on ATS medium under long day conditions at 20°C. Three biological replicates were measured, each in two technical replicates. Error bars represent SE. Transcript level of genes labeled with asterisks were under the detection limit in the analyzed plant organs.

Supplemental Table S1. Identifiers of F-box kelch proteins in *A. thaliana*, *P. trichocarpa*, *V. vinifera*, *O. sativa*, *S. bicolor*, *S. moellendorffii* and *P. patens*.

Arabidopsis	Populus	Vitis	Oryza	Sorghum	Selaginella	Physcomitrella
AT1G14330	Pop|174433	GSV00121001	Os01g33490	Sb01g013220	Selm|115581	jgi|Phypa1_1|101961
AT1G15670	Pop|177961	GSV02287001	Os01g47050	Sb01g013240	Selm|121243	jgi|Phypa1_1|104453
AT1G16250	Pop|230616	GSV02498001	Os01g50840	Sb01g022240	Selm|14013	jgi|Phypa1_1|108027
AT1G19460	Pop|244788	GSV02750001	Os01g69940	Sb01g022460	Selm|174189	jgi|Phypa1_1|114815
AT1G19470	Pop|265449	GSV02843001	Os02g02350	Sb01g045700	Selm|23216	jgi|Phypa1_1|118316
AT1G19930	Pop|267446	GSV02903001	Os02g05700	Sb01g046015	Selm|272238	jgi|Phypa1_1|126823
AT1G22040	Pop|274431	GSV07630001	Os02g10850	Sb02g001990	Selm|33540	jgi|Phypa1_1|131411
AT1G23390	Pop|283960	GSV13963001	Os02g11790	Sb02g002025	Selm|33948	jgi|Phypa1_1|137266
AT1G26930	Pop|287991	GSV15284001	Os02g15950	Sb02g003160	Selm|402181	jgi|Phypa1_1|139248
AT1G27420	Pop|298158	GSV16869001	Os02g21110	Sb02g005040	Selm|403983	jgi|Phypa1_1|14114
AT1G30090	Pop|420602	GSV17315001	Os02g30210	Sb02g005880	Selm|404324	jgi|Phypa1_1|153643
AT1G31350	Pop|547623	GSV19396001	Os02g35530	Sb02g025486	Selm|404826	jgi|Phypa1_1|156376
AT1G51550	Pop|547631	GSV24520001	Os02g36520	Sb02g032340	Selm|405137	jgi|Phypa1_1|158495
AT1G55270	Pop|548662	GSV24761001	Os02g51350	Sb02g042690	Selm|405262	jgi|Phypa1_1|159848
AT1G60570	Pop|548664	GSV25445001	Os03g07160	Sb03g030090	Selm|406718	jgi|Phypa1_1|159974
AT1G61540	Pop|549362	GSV26849001	Os03g07530	Sb03g041500	Selm|407049	jgi|Phypa1_1|159978
AT1G67480	Pop|551335	GSV26855001	Os03g30160	Sb03g041730	Selm|409427	jgi|Phypa1_1|160103
AT1G68050	Pop|552235	GSV26967001	Os04g31120	Sb04g001090	Selm|411128	jgi|Phypa1_1|160232
AT1G74510	Pop|553842	GSV28309001	Os04g52830	Sb04g003660	Selm|411144	jgi|Phypa1_1|161137
AT1G76920	Pop|555218	GSV29589001	Os04g57290	Sb04g007310	Selm|412518	jgi|Phypa1_1|162266
AT1G80440	Pop|558147	GSV30594001	Os06g39370	Sb04g009700	Selm|417121	jgi|Phypa1_1|162989
AT2G02870	Pop|559358	GSV31346001	Os06g44500	Sb04g009920	Selm|421271	jgi|Phypa1_1|163528
AT2G18915	Pop|559574	GSV31580001	Os06g47890	Sb04g020510	Selm|421284	jgi|Phypa1_1|163752
AT2G20380	Pop|561211	GSV32323001	Os06g49750	Sb04g023200	Selm|422132	jgi|Phypa1_1|164205
AT2G21680	Pop|561242	GSV32333001	Os07g02910	Sb04g023750	Selm|422192	jgi|Phypa1_1|164284
AT2G21950	Pop|563452	GSV32404001	Os07g03100	Sb04g027910	Selm|424145	jgi|Phypa1_1|166753
AT2G22030	Pop|564672	GSV33280001	Os07g05880	Sb05g002260	Selm|426714	jgi|Phypa1_1|166966
AT2G22050	Pop|565042	GSV33282001	Os07g47650	Sb05g006950	Selm|429669	jgi|Phypa1_1|167883
AT2G24540	Pop|566051	GSV33571001	Os08g13360	Sb05g006960	Selm|429850	jgi|Phypa1_1|168336
AT2G29600	Pop|572245	GSV34447001	Os09g38300	Sb05g021030	Selm|431561	jgi|Phypa1_1|169046

Arabidopsis	Populus	Vitis	Oryza	Sorghum	Selaginella	Physcomitrella
AT2G29770	Pop|572337	GSV34454001	Os10g04890	Sb05g023750	Selm|438121	jgi|Phypa1_1|169120
AT2G29780	Pop|583883	GSV34587001	Os10g21930	Sb06g012290	Selm|441635	jgi|Phypa1_1|169426
AT2G29800	Pop|589736	GSV34781001	Os10g24900	Sb06g025030	Selm|448225	jgi|Phypa1_1|169940
AT2G29810	Pop|592319	GSV37006001	Os10g25210	Sb06g028820	Selm|55890	jgi|Phypa1_1|171546
AT2G29820	Pop|597156	GSV37841001	Os10g26990	Sb06g032150	Selm|65366	jgi|Phypa1_1|172502
AT2G29830	Pop|649911	GSV38104001	Os11g04330	Sb06g033350	Selm|75526	jgi|Phypa1_1|172546
AT2G29860	Pop|651336		Os11g14140	Sb06g033750	Selm|766041	jgi|Phypa1_1|172882
AT2G41360	Pop|658140		Os11g34460	Sb07g002320	Selm|78419	jgi|Phypa1_1|180856
AT2G44030	Pop|708739		Os12g04130	Sb07g006910	Selm|79476	jgi|Phypa1_1|181624
AT2G44130	Pop|754910			Sb10g023140	Selm|83069	jgi|Phypa1_1|188742
AT2G44630	Pop|756767			Sb10g026080	Selm|85806	jgi|Phypa1_1|188796
AT2G44700	Pop|758312			Sb10g026580	Selm|87207	jgi|Phypa1_1|189687
AT3G06570	Pop|758319			Sb10g028340	Selm|88328	jgi|Phypa1_1|201289
AT3G08810	Pop|762216			Sb10g029710	Selm|92558	jgi|Phypa1_1|202273
AT3G10510	Pop|763659				Selm|92689	jgi|Phypa1_1|229126
AT3G24610	Pop|764261				Selm|92722	jgi|Phypa1_1|229344
AT3G24760	Pop|768560					jgi|Phypa1_1|231395
AT3G27150	Pop|771222					jgi|Phypa1_1|233086
AT3G27910	Pop|780347					jgi|Phypa1_1|233535
AT3G43710	Pop|780375					jgi|Phypa1_1|233728
AT3G46050	Pop|783326					jgi|Phypa1_1|233823
AT3G59940	Pop|798553					jgi|Phypa1_1|234202
AT3G61350	Pop|800124					jgi|Phypa1_1|234490
AT3G61590	Pop|801458					jgi|Phypa1_1|234671
AT3G63220	Pop|805659					jgi|Phypa1_1|23672
AT4G02310	Pop|807034					jgi|Phypa1_1|23835
AT4G03030	Pop|807217					jgi|Phypa1_1|44026
AT4G11750	Pop|809263					jgi|Phypa1_1|44304
AT4G11770	Pop|811754					jgi|Phypa1_1|45289
AT4G14905	Pop|822050					jgi|Phypa1_1|45319
AT4G19330	Pop|825819					jgi|Phypa1_1|5127
AT4G19865	Pop|830083					jgi|Phypa1_1|63719

Arabidopsis	Populus	Vitis	Oryza	Sorghum	Selaginella	Physcomitrella
AT4G19870	PtI002296					jgi|Phypa1_1|63738
AT4G23580	PtVII000004					jgi|Phypa1_1|68326
AT4G25710	PtX002172					jgi|Phypa1_1|70860
AT4G29370	Pt170000007					jgi|Phypa1_1|90500
AT4G33900	PtVIII000539					jgi|Phypa1_1|91322
AT4G34170	Pt129000020					jgi|Phypa1_1|96028
AT4G35120						jgi|Phypa1_1|96502
AT4G38940						jgi|Phypa1_1|97006
AT4G39240						jgi|Phypa1_1|98858
AT4G39290						
AT4G39550						
AT4G39560						
AT4G39570						
AT4G39580						
AT4G39590						
AT4G39600						
AT4G39753						
AT4G39756						
AT4G39760						
AT5G02980						
AT5G02990						
AT5G03000						
AT5G03020						
AT5G07610						
AT5G15710						
AT5G26960						
AT5G28160						
AT5G28180						
AT5G38670						
AT5G38680						
AT5G39560						
AT5G40680						

Arabidopsis	Populus	Vitis	Oryza	Sorghum	Selaginella	Physcomitrella
AT5G42350						
AT5G42360						
AT5G43190						
AT5G48980						
AT5G48990						
AT5G49000						
AT5G51250						
AT5G57360						
AT5G60570						

Supplemental Table S2. Number of F-box kelch proteins in non-plant model species

Species	Number of FBKs	Number of kelch repeats (Pfam)	Protein ID
Bacteria	-	-	-
Saccharomyces cerevisae	-	-	-
Chlamydomonas reinhardtii	1	3	EDP09183[a]
Caenorhabditis elegans	1	3	Q9N3K6[b]
Drosophila melanogaster	1	3	Q9W281[b]
Mus Musculus	1	3	Q6PDJ6[b]
Homo sapiens	1	3	Q6P3S6[b]

[a]GenBank ID; [b]Swiss Prot ID

Supplemental Table S3: Identifiers of F-box proteins with F-box associated domains in *A. thaliana*, *P. trichocarpa, V. vinifera*, *O. sativa*, *S. bicolor*, *S. moellendorffii* and *P. patens.*

Arabidopsis	Populus	Vitis	Oryza	Sorghum	Selaginella	Physcomitrella
AT1G09650	Pop|241644	GSV02287001*	Os02g10600	Sb01g003460	Selm|428410	jgi|Phypa1_1|163116
AT1G10890	Pop|246916	GSV26022001	Os02g33840	Sb01g013220*	Selm|413145	jgi|Phypa1_1|164205*
AT1G11620	Pop|547750	GSV26967001*	Os02g35560	Sb01g013240*	Selm|33948*	jgi|Phypa1_1|234287
AT1G11810	Pop|548688	GSV33571001	Os03g25640	Sb01g018980		jgi|Phypa1_1|234728
AT1G12170	Pop|548689	GSV33582001	Os03g46690	Sb01g031390		jgi|Phypa1_1|65071
AT1G12190	Pop|549801		Os04g11450	Sb01g034970		jgi|Phypa1_1|90500*
AT1G12870	Pop|560159		Os04g11660	Sb01g037880		jgi|Phypa1_1|91913
AT1G13200	Pop|563457		Os04g11790	Sb02g001040		
AT1G24793	Pop|565298		Os04g50200	Sb02g002025*		
AT1G24880	Pop|568920		Os05g02570	Sb02g005870		
AT1G25141	Pop|569113		Os05g08010	Sb02g005880*		
AT1G30780	Pop|569545		Os05g08350	Sb02g005890		
AT1G30790	Pop|569549		Os05g08440	Sb02g008113		
AT1G30920	Pop|570279		Os05g08460	Sb02g023440		
AT1G30925	Pop|571268		Os06g07380	Sb02g027685		
AT1G30930	Pop|571296		Os06g07390	Sb03g044080		
AT1G30935	Pop|574752		Os06g07460	Sb04g000800		
AT1G31000	Pop|575938		Os07g08570	Sb04g003010		
AT1G31080	Pop|579428		Os07g09710	Sb04g006790		
AT1G31090	Pop|581757		Os07g09814	Sb04g009700*		
AT1G32140	Pop|581764		Os07g09870	Sb04g025085		
AT1G32420	Pop|585979		Os07g13870	Sb04g026045		
AT1G32430	Pop|587549		Os07g13890	Sb05g020470		
AT1G32660	Pop|590131		Os07g16420	Sb05g025730		
AT1G33010	Pop|590133		Os07g16800	Sb05g025750		
AT1G33020	Pop|590935		Os07g35050	Sb06g027040		
AT1G33530	Pop|592321		Os07g35060	Sb08g003880		
AT1G46840	Pop|597059		Os08g10340	Sb08g015610		
AT1G46984	Pop|666139		Os08g36960	Sb08g021860		
AT1G47340	Pop|241644		Os09g20650	Sb08g021900		

Arabidopsis	Populus	Vitis	Oryza	Sorghum	Selaginella	Physcomitrella
AT1G47390	Pop|752836		Os09g27570	Sb09g027720		
AT1G47730	Pop|753649		Os09g30180	Sb09g030410		
AT1G47765	Pop|754910*		Os09g34200	Sb10g010900		
AT1G47790	Pop|756767*		Os10g04850	Sb10g024600		
AT1G47800	Pop|761635		Os10g25210*			
AT1G47810	Pop|761790		Os10g25660			
AT1G48060	Pop|763809		Os12g03440			
AT1G50870	Pop|764347		Os12g06740			
AT1G50880	Pop|764712		Os06g0170866			
AT1G51290	Pop|765277					
AT1G51320	Pop|766270					
AT1G52490	Pop|770387					
AT1G53370	Pop|771222*					
AT1G53550	Pop|775680					
AT1G53790	Pop|783326					
AT1G54550	Pop|786330					
AT1G55070	Pop|787092					
AT1G58090	Pop|799299					
AT1G59680	Pop|801694					
AT1G60370	Pop|805278					
AT1G61060	Pop|807217*					
AT1G62270	Pop|808297					
AT1G65990						
AT1G66490						
AT1G67130						
AT1G67450						
AT1G67455						
AT1G70380						
AT1G70390						
AT1G70960						

Arabidopsis	Populus	Vitis	Oryza	Sorghum	Selaginella	Physcomitrella
AT1G70970						
AT1G71320						
AT1G76830						
AT1G77650						
AT2G02890						
AT2G04920						
AT2G07140						
AT2G13130						
AT2G14710						
AT2G15640						
AT2G16220						
AT2G16450						
AT2G16810						
AT2G17310						
AT2G17830						
AT2G18780						
AT2G19630						
AT2G21930						
AT2G23160						
AT2G27520						
AT2G31470						
AT2G33655						
AT2G34280						
AT2G38590						
AT2G40910						
AT2G40920						
AT2G40925						
AT2G43260						
AT2G43440						
AT3G04660						

Arabidopsis	Populus	Vitis	Oryza	Sorghum	Selaginella	Physcomitrella
AT3G06240						
AT3G07870						
AT3G08750						
AT3G10240						
AT3G10430						
AT3G10790						
AT3G13680						
AT3G13820						
AT3G13830						
AT3G16210						
AT3G16555						
AT3G16580						
AT3G16590						
AT3G16740						
AT3G16820						
AT3G16880						
AT3G17265						
AT3G17280						
AT3G17320						
AT3G17480						
AT3G17490						
AT3G17500						
AT3G17530						
AT3G17540						
AT3G17560						
AT3G17570						
AT3G17620						
AT3G17710						
AT3G18320						
AT3G18330						

Arabidopsis	Populus	Vitis	Oryza	Sorghum	Selaginella	Physcomitrella
AT3G18340						
AT3G18910						
AT3G18980						
AT3G19410						
AT3G19470						
AT3G19560						
AT3G19880						
AT3G19890						
AT3G20030						
AT3G20690						
AT3G20710						
AT3G21120						
AT3G21130						
AT3G21170						
AT3G21410						
AT3G22350						
AT3G22421						
AT3G22650						
AT3G22700						
AT3G22710						
AT3G22720						
AT3G22730						
AT3G22870						
AT3G22940						
AT3G23260						
AT3G23420						
AT3G23880						
AT3G23960						
AT3G24580						
AT3G25460						

Arabidopsis	Populus	Vitis	Oryza	Sorghum	Selaginella	Physcomitrella
AT3G44120						
AT3G44130						
AT3G47020						
AT3G47030						
AT3G47150						
AT3G49450						
AT3G49510						
AT3G49520						
AT3G49980						
AT3G52320						
AT3G57580						
AT3G57590						
AT3G59610						
AT3G61340						
AT4G04690						
AT4G05080						
AT4G09190						
AT4G09790						
AT4G09870						
AT4G10740						
AT4G11590						
AT4G12560						
AT4G17200						
AT4G17780						
AT4G19930						
AT4G19940						
AT4G21240						
AT4G29970						
AT4G33160						
AT4G33290						

Arabidopsis	Populus	Vitis	Oryza	Sorghum	Selaginella	Physcomitrella
AT4G38870						
AT5G07610*						
AT5G10340						
AT5G15660						
AT5G15670						
AT5G18160						
AT5G36200						
AT5G36730/ AT5G36820						
AT5G37040						
AT5G38810						
AT5G41490						
AT5G41500						
AT5G41510						
AT5G42430						
AT5G42460						
AT5G47300						
AT5G50220						
AT5G51000						
AT5G52610						
AT5G52620						
AT5G60560						
AT5G62060						
AT5G62510						
AT5G62660						
AT5G65850						

* F-box proteins with F-box associated domain and kelch repeats.

Supplemental Table S4: Comparison of three tree topologies obtained with three different algorithms (NJ=Neighbor-Joining, Bayesian and ML=Maximum Likelihood) using Shimodaira-Hasegawa (Shimodaira and Hasegawa, 1999) and one-sided Kishino-Hasegawa (1sKH, Kishino and Hasegawa, 1989) tests, implemented in Treepuzzle (Schmidt and von Haeseler, 2007). In addition, a Chi-square test was performed to compare the likelihoods (l) of the three trees to the best tree (in this case the ML tree). The ML and NJ trees have the same likelihood.

Tree	l	∆l	S.E.	p1-skh	p-SH	2∆l	Chi-square	p-value
NJ	-30957.15	0	0.0024	1	0.737	0	0	0
Bayesian	-31069.27	112.12	22.7059	0	0	224.24	0.406	0.03
ML	-30957.15	0	best tree	1	1	0	0	0

Schmidt HA, von Haeseler A (2007) Maximum-likelihood analysis using TREE-PUZZLE. Curr Prot Bioinformatics **Chapter 6**: Unit 6.6

Supplemental Table S5. Number of unstable, stable, ancient and superstable FBKs in *A. thaliana*, *V. vinifera*, *P. trichocarpa*, *O. sativa*, *S. bicolor*, *S.moellendorffii* and *P. patens*.

Species	Number of unstable FBKs	Number of stable FBKs	Number of ancient FBKs	Number of superstable FBKs	Total number of FBKs
Arabidopsis thaliana	66	14	12	11	103
Vitis vinifera	0	15	9	12	36
Populus trichocarpa	0	21	30	17	68
Oryza sativa	0	11	15	13	39
Sorghum bicolor	0	18	16	10	44
Selaginella moellendorffii	5	16	11	14	46
Physcomitrella patens	19	20	5	27	71

Supplemental Table S6. Sequences of q-RT PCR primers

Primer	Sequence
AT1G14330_F	5’ ACTGAGATACCGGAAATGTCGC 3’
AT1G14330_R	5’ TCAGCATGATCAGCAGCATACA 3’
AT1G26930_F	5’ AGAGATTGCGGTTTTAGCGG 3’
AT1G26930_R	5’ CATCCATAAACACACCGGAACA 3’
AT1G74510_F	5’ AGCTTTATGCTGCGAATTACGC 3’
AT1G74510_R	5’ CACTAACTGATCCCCACAAGCC 3’
AT2G02870_F	5’ TGATCACGCCGATATGGAAGT 3’
AT2G02870_R	5’ AGCAAGTCCCCATCCGTTTAC 3’
AT3G27150_F	5’ CGTGTTGGACGATGTTTGACA 3’
AT3G27150_R	5’ CGCAAAGCGATTCTTTATCTCC 3’
AT5G40680_F	5’ CGTATTGTGGTGTGGCGATA 3’
AT5G40680_R	5’ CTTGATTCCTCCAGCGAAAA 3’
AT5G60570_F	5’ ATGGTGGACTCGTCAAACGGT 3’
AT5G60570_R	5’ CAAGAATTCACCACAATGCCCT 3’